# Technical Note

## 1971-34

S. Rosenbaum
L. W. Bowles

## Clutter Return
from Vegetated Areas

10 September 1971

# Lincoln Laboratory

MASSACHUSETTS INSTITUTE OF TECHNOLOGY

Lexington, Massachusetts
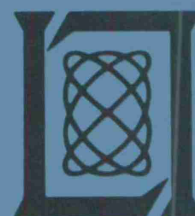
Approved for public release; distribution unlimited.

MASSACHUSETTS INSTITUTE OF TECHNOLOGY

LINCOLN LABORATORY

# CLUTTER RETURN FROM VEGETATED AREAS

*S. ROSENBAUM*

*Consultant*

*L. W. BOWLES*

*Group 68*

TECHNICAL NOTE 1971-34

10 SEPTEMBER 1971

LEXINGTON                                                   MASSACHUSETTS

## ABSTRACT

The objective of this report is the presentation of an analytical-
stochastic model capable of predicting relevant statistical scattering
features of electromagnetic waves propagating within vegetated environ-
ments. The propagation phenomena are described by formulating the
scattering associated with random permittivity fluctuations superimposed
on a lossy deterministic background slab. The mean backscattered power,
its variance and one-point distribution are calculated. The spectral
characteristics of clutter from windblown foliage are investigated using
two models; one presuming the velocity field to constitute a multi-variate
normal process and another presuming the scatterer's motion to be quasi-
harmonic over limited time segments.

# CONTENTS

# CLUTTER RETURN FROM VEGETATED AREAS

## A. INTRODUCTION

The objective of this report is the presentation of an analytical-stochastic model capable of predicting relevant statistical scattering features of EM waves propagating within vegetated environments. Of interest are such features as the spectral content of the clutter return as well as the received power (and related statistics) from gated range-cells. Other pertinent wave features not discussed but which can be pursued within the framework of the suggested model are mentioned at the end of this section.

The forest constitutes a complicated transmission medium. Its characterizing parameters (i.e., permittivity and conductivity) are random functions of space and time. Furthermore, its interfaces, particularly the air-vegetation interface which may play a major role in the transmission process (e.g., through its support of a "lateral" wave) are "rough". Further discussion of the stochastic character of the interfaces and the corresponding effects on the EM radiation is omitted at present. This by no means implies lack of significance. It is the surface roughness which conceivably causes the deterioration of the "lateral" wave.

The forest constitutes an ensemble of various scattering constituents. Fortunately, not all influence the EM characteristics in the same manner. The outstanding difference between

these scatterers is their physical dimension compared to the wavelength of the incident radiation.

Small-scale scatterers are characterized by small scattering cross-section. Their relative contributions to the scattered field (the elementary scattering event is virtually isotropic) are expected to be small. The presence of small-scale scatterers, however, is extremely significant because of the modifications they impose upon the _effective_ propagation features of both the incident as well as the scattered radiation. Multiple-scattering events experienced by either the incident wave or by the wave back-scattered to the receiving antenna have a two-fold effect[1-3]:

(a)     Scattering losses (additional to the ever-present absorption losses) reduce the efficiency of the channel and must be properly accounted for. The medium which effectively describes the propagation of the mean wave predicts losses which may become considerably higher than those anticipated from absorption alone.

(b)     In addition to the scattering losses the mean wave experiences an effective slowdown. The medium seems denser than that expected in the absence of scattering.

The small-scale scattering effects indicated above are accounted for by a proper choice of the effective background permittivity and conductivity. The relative contributions of small-scale scatterers to the _scattered-wave_ may not be small

2

throughout the contributing spectrum. Specifically, attention must be paid to the spectral "tail" region to which small-scale scatterers may, despite their small cross section, contribute significantly since they may attain relatively high velocities.

The effects of scattering centers contributing to the bulk of the back-scattered energy cannot be accounted for in an analogously simple manner since the scattering is controlled by the random <u>deviations</u> of the (complex) permittivity function from the background, a more accurate description of the space-time medium fluctuations is called for. First order scattering theories highlight the need for more detailed knowledge; that contained in the space-time auto and cross correlation functions of the pertinent electromagnetic parameters.

At relatively low frequencies (say below 100 MHz) virtually all the forest constituents are in the small-scale category. The effect of the scattering on the propagation characteristics of the <u>mean</u> wave is totally describable by an effective background selection leading to the familiar deterministic "forest-slab" model[4,5]. The scattered wave is both small in magnitude and inconsequential to applications at these frequencies and thus has been totally ignored. As the frequency rises to the range which includes UHF and L-band, the scattered wave can no longer be ignored. The small-scale scattering constituents cannot be ignored either; their determination of the background slab (over which the random

3

fluctuations are to be superimposed) is of utmost importance.
At still higher frequencies (say X-band and beyond) most scat-
terers appear to be large-scale. Coherent background effects no
longer exist and all scattering centers must be regarded as
belonging to the "fluctuation" spectrum.

Figure 1 describes the physical configuration consistently
with previously presented arguments. The medium is modeled as a
slab of average height h (which may not coincide with the average
height concluded from visual observations); a complex background
permittivity $\epsilon_{eff} = \epsilon_2$ which is presumed constant (more precise
models may necessitate more complicated plan-stratified or possibly
anisotropic backgrounds); and permittivity fluctuations ($\epsilon$ ($\underline{r}$,t) )
which are random functions of space and time with supposedly
known two-point space-time correlation functions. $\epsilon_2$ is neces-
sarily complex accounting for absorption as well as scattering
losses. The ground is taken to be a perfect reflector (a
reasonable assumption for horizontally polarized waves). As
mentioned above, the random nature of both vegetation-air and
vegetation-ground interfaces is disregarded at present. The
forthcoming analysis presumes the dominance of geometric-optical
contributions to both the incident as well as the backscattered
radiation. This is not the case under a wide variety of circum-
stances such as (a) antenna within the vegetation (or within few
wavelengths above it), (b) range cell in the shadow region of the

4

geometric-optical refracted wave due to hilly terrain, etc. It can be assumed that the coupling between the interfaces is small (a reasonable assumption in view of the prevailing scattering and absorption losses). This allows one to treat the forest as a half-space, with ground effects accounted for as the single and double reflections illustrated in Figs. 8a, b. These ground reflections render the determination of the range-cell's location uncertain. However, the introduced errors are expected to be minimal in the present context.

It is anticipated that the solution of the random scattering problem (i.e., the determination of the analytical relations between the presumably known forest parameters and the pertinent wave statistics) via "distorted wave Born approximation" would provide acceptable accuracy under the prevailing circumstances.

Contributions to the crossed polarized wave do, in general, stem from both coherent background effects (reflection, refraction and diffraction) as well as random multiple-scattering events (first order description of the cross polarized field is provided by the second order Born approximation[6]). Since it is a single-scatter mechanism which is believed to dominate, depolarization due to random scattering is presumably insignificant. Coherent refraction and diffraction (giving rise to a lateral-wave) are likely to become major contributors to the crossed-polarized wave. However, the rather small discontinuity at the air-forest inter-

5

face suggests that the overall effect is small. This is not to say that the original polarization dominates everywhere. For example, near the ground, or at minima occurring due to destructive interference of the horizontally polarized wave, the vertical crossed-polarized component may dominate locally despite its smallness. The total amplitude of the incident field will be small and as a result the backscatter from these spatial regions is negligible.

Section B describes the physical configuration and formulates the scattering problem associated with the random permittivity fluctuations superimposed on a lossy deterministic background slab. The background problem is discussed in Section C, starting from the exact field solutions. Asymptotic, geometric-optical forms are derived, tailored to the specific parameter range; relevant to the prevailing experimental conditions. Conditions, restricting the validity of the geometric-optical filters are discussed and a comparison with possible "lateral"-wave contributions is given. In Section D (and in the Appendix) we derive expressions describing the scattered field consistently with the distorted wave Born approximation and the observations made in Sections A and B. The mean received power, its variance and one-point distribution as well as the field's temporal correlation associated with the clutter return are calculated. The clutter's spectral characteristics are investigated in Section E. Two

6

models, one presuming the velocity field to constitute a multivariate normal process and another presuming the scatterer's motion to be quasi-harmonic over limited time segments are discussed.

Certain relevant aspects not presented in this report but which can be readily described within the general framework of the proposed model are mentioned below:

(a)     Situations in which the geometric-optical field no longer constitutes a major contribution. This is the case whenever the transmitting and/or receiving antennas are situated within (or slightly above) the vegetation. A similar situation arises whenever the range-cell is situated in the shadow region of the refracted wave, owing, say, to hilly terrain. The "lateral" wave constitutes the major channel.

(b)     Distribution laws of the scattered field. Amplitude (power) fluctuations and related two-point statistics associated with target and clutter returns.

(c)     Effects of vegetation (random slab) on target spectrum.

(d)     Smoothing effects owing to finite aperture of the receiving antenna and/or finite extent the target.

7

(e)     Generalization to bi-static situations.

(f)     Pulse-shape distortion and the resulting range-
cell diffusion.

The analytical details of the model are, at times, tailored
to the specific parameter range of interest.  Many of these
restrictions may be waived if the need arises under varying
circumstances.

B.     FORMULATION OF THE PROBLEM

The pertinent physical configuration is described in
Fig. 1.  Heuristic arguments in support of the random slab model
have been presented in a previous interim report and the
Introduction above.  It should be noted that the permittivity
$\epsilon_2 + \epsilon(\underline{r}, t)$ is generally complex reflecting absorption as well
as scattering losses within the slab region.  Since the
absorption and more so the random scattering constitute frequency
sensitive phenomena it could be anticipated that both $\epsilon_2$ and
$\epsilon(\underline{r}, t)$ (and its characterizing statistics) are frequency-
dependent (dispersive) as well.  Also, the assumption of perfect
ground conductivity while generally valid for the horizontal
polarization is unsatisfactory for the vertical polarization.

The propagation and scattering characteristics of the EM
waves are determined by Maxwell's equations:

8

$\epsilon_0, \mu_0$

$18-D0-7201(1)$

$\epsilon_g, \sigma_g, \mu_g$

$z$

$\epsilon_1 = \epsilon_0, \mu_0$    $\underline{J}_1$

1
2

0

$\epsilon_2 + \epsilon(\underline{r}, t), \mu_2 = \mu_0$

$<\epsilon(\underline{r}, t)> = 0$

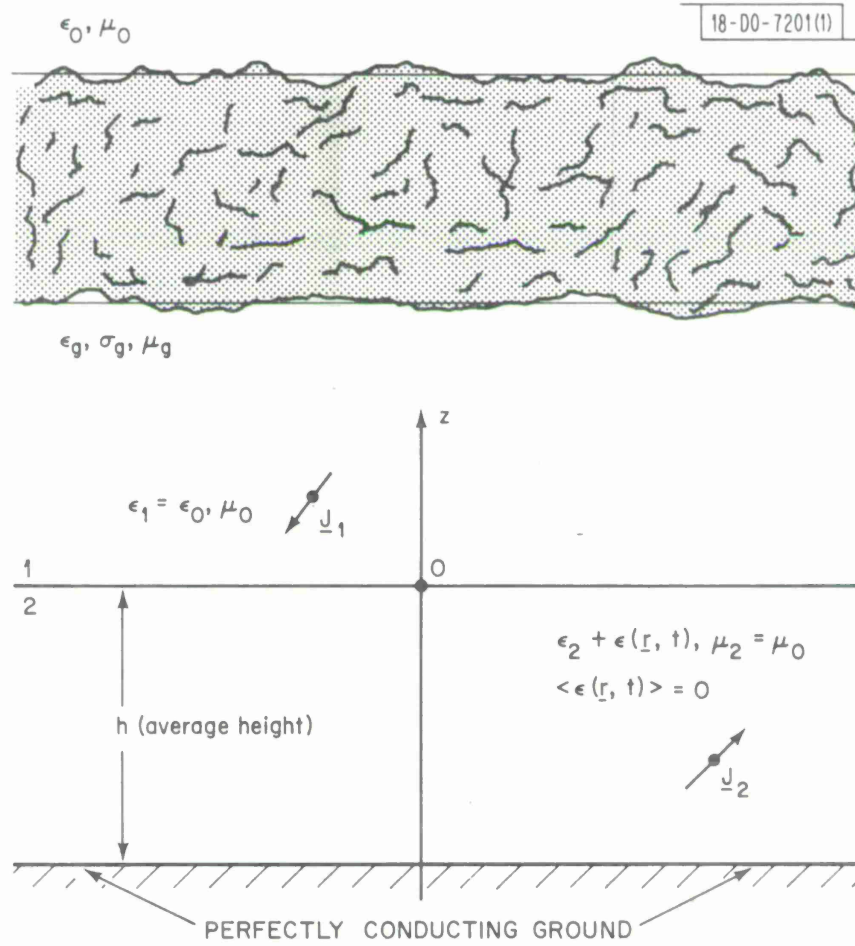$h$ (average height)

$\underline{J}_2$

PERFECTLY CONDUCTING GROUND

Fig. 1.  Physical configuration.

$$\nabla \times H_1 = \epsilon_1 \frac{\partial \widehat{\underline{E}}_1}{\partial t} + \widehat{\underline{J}}_1 \qquad \nabla \times \widehat{\underline{H}}_2 = \epsilon_2 \frac{\partial \widehat{\underline{E}}_2}{\partial t} + \frac{\partial}{\partial t} (\epsilon \, \widehat{\underline{E}}_2) + \widehat{\underline{J}}_2 \qquad (1)$$

$$\nabla \times \widehat{\underline{E}}_1 = - \mu_o \frac{\partial \widehat{\underline{H}}_1}{\partial t} \qquad \nabla \times \widehat{\underline{E}}_2 = - \mu_o \frac{\partial \widehat{\underline{H}}_2}{\partial t} \qquad (2)$$

together with the continuity conditions

$$\widehat{\underline{E}}_{1t} = \widehat{\underline{E}}_{2t} \, , \qquad \widehat{\underline{H}}_{1t} = \widehat{\underline{H}}_{2t} \qquad (3)$$

at the interface and a causality condition which in the steady-state case becomes the radiation-condition at $r \to \infty$.

It is presumed that the temporal medium variations, characterized by the correlation time $\tau_c$, are slow compared to these of the wave, i.e., $\omega_o \tau_c \gg 1$ where $\omega_o$ is the angular frequency of the presumedly monochromatic transmitter.

Let,

$$\underline{E}_{1 \atop 2} (\underline{r}, t) = \mathrm{Re} \left[ \underline{E}_{1 \atop 2} (\underline{r}, t) \, e^{j \omega_o t} \right] \qquad (4)$$

$$\underline{H}_{1 \atop 2} (\underline{r}, t) = \mathrm{Re} \left[ \underline{H}_{1 \atop 2} (\underline{r}, t) \, e^{j \omega_o t} \right] \qquad (5)$$

$$\underline{J}_{1 \atop 2} (\underline{r}, t) = \mathrm{Re} \left[ \underline{J}_{1 \atop 2} (\underline{r}) \, e^{j \omega_o t} \right] \qquad (6)$$

10

(Note: since the source is taken to be monochromatic $\underline{J}_{1,2}$ is time independent.) The substitution of Eqs. (4-6) into Maxwell's equations (1,2) results in:

$$\nabla \times \underline{E}_1 = -j\omega_o\mu_o \left(1 + \frac{1}{j\omega_o} \frac{\partial}{\partial t}\right) \underline{H}_1 + \underline{J}_1 \, (r) \tag{7}$$

$$\nabla \times \underline{H}_1 = j\omega_o\epsilon_1 \left(1 + \frac{1}{j\omega_o} \frac{\partial}{\partial t}\right) \underline{E}_1 \tag{8}$$

$$\nabla \times \underline{E}_2 = -j\omega_o\mu_o \left(1 + \frac{1}{j\omega_o} \frac{\partial}{\partial t}\right) \underline{H}_2 \tag{9}$$

$$\nabla \times \underline{H}_2 = j\omega_o \left(1 + \frac{1}{j\omega_o} \frac{\partial}{\partial t}\right) \left[\epsilon_2 \underline{E}_2 + \epsilon \underline{E}_2\right] + \underline{J}_2 \, (r) \tag{10}$$

from which the following vector wave equations are readily derived:

$$\nabla \times \nabla \times \underline{E}_1 - k_1^2 \left(1 + \frac{1}{j\omega_o} \frac{\partial}{\partial t}\right)^2 \underline{E}_1 = j\omega_o\mu_o \underline{J}_1 \tag{11}$$

$$\nabla \times \nabla \times \underline{E}_2 - k_2'^2 \left(1 + \frac{1}{j\omega_o} \frac{\partial}{\partial t}\right)^2 \underline{E}_2 = j\omega_o\mu_o \underline{J}_2 + \omega_o^2\mu_o \left(1 + \frac{1}{j\omega_o} \frac{\partial}{\partial t}\right)\left(\epsilon \underline{E}_2\right) \tag{12}$$

where $\quad k_{1 \atop 2}^2 = \omega_o^2 \, \mu_o \, \epsilon_{1 \atop 2} \quad .$

Terms associated with the slow temporal derivative may be safely omitted due to the smallness of $\left(\omega_o \tau_c\right)^{-1} \approx \frac{\Delta\omega}{\omega_o} \ll 1$. (here $\Delta\omega$ denotes the frequency deviation of the wave from $\omega_o$).

11

For example, comparing the terms $|\epsilon \underline{E}_2|$ with $|\frac{2}{j\omega_0} \frac{\partial}{\partial t} (\epsilon \underline{E}_2)|$ one has

$$|\frac{2}{j\omega_0} \frac{\partial}{\partial t} (\epsilon \underline{E}_2)| \ / \ |\epsilon \underline{E}_2| = |\frac{2}{j\omega_0} (\frac{\partial \epsilon}{\partial t} \underline{E}_2 + \epsilon \frac{\partial \underline{E}_2}{\partial t})| / |\epsilon \underline{E}_2| \approx$$

$$(\omega_0 \tau_c)^{-1} + \frac{\Delta \omega}{\omega_0} \langle\langle \ 1 \tag{13}$$

consequently, we may take

$$1 + \frac{1}{j\omega_0} \ \frac{\partial}{\partial t} \approx 1$$

and equations (11, 12) reduce to

$$\nabla \times \nabla \times \underline{E}_1 - k_1^2 \ \underline{E}_1 = -j\omega_0 \mu_0 \ \underline{J}_1 \tag{14}$$

$$\nabla \times \nabla \times \underline{E}_2 - k_2^2 \ \underline{E}_2 = -j\omega_0 \mu_0 \ \underline{J}_2 + \omega_0^2 \mu_0 \ \epsilon \ \underline{E}_2 \quad , \ \epsilon = \epsilon \ (\underline{r},t) \tag{15}$$

in which time appears as a parameter.

Let $\underline{\underline{G}}_{1,2}$ denote the Dyadic Green's function defined by the equations,

$$\nabla \times \nabla \times \underline{\underline{G}}_1 - k_1^2 \ \underline{\underline{G}}_1 = 0 \qquad\qquad z \rangle 0 \tag{16}$$

$$\nabla \times \nabla \times \underline{\underline{G}}_2 - k_2^2 \ \underline{\underline{G}}_2 = \underline{\underline{I}}\delta \ (\underline{r}-\underline{r}') \quad -h \langle z \langle 0 \tag{17}$$

the radiation condition at infinite and the appropriate continuity conditions at $z = 0$. Here, $\underline{\underline{I}}$ denotes the unit dyadic.

12

Let $\underline{E}_{1,2}^{(0)} = \underline{E}_{1,2}(\varepsilon=0)$ and $\underline{E}_{1,2s} = \underline{E}_{1,2} - \underline{E}_{1,2}^{(0)}$ denote

the unperturbed (background) and the scattered waves, respectively.
From the basic definitions and Eqs. (14, 15) one obtains:

$$\nabla \times \nabla \times \underline{E}_{1s} - k_1^2 \, \underline{E}_{1s} = 0 \tag{18}$$

$$\nabla \times \nabla \times \underline{E}_{2,s} - k_2^2 \, \underline{E}_{2s} = \omega_o^2 \, \mu_o \, \varepsilon(\underline{r},t) \, \underline{E}_2 \tag{19}$$

which may via Eqs. (16, 17) be converted to the convenient
integral forms

$$\underline{E}_{1s} = \omega_o^2 \, \mu_o \int_{V_s} d^3 \, r_1 \, \varepsilon(\underline{r}_1,t) \, \underline{G}_1 \, (\underline{r}, \, \underline{r}_1) \cdot \underline{E}_2 \, (\underline{r}_1,t) \tag{20}$$

$$\underline{E}_{2s} = \omega_o^2 \, \mu_o \int_{V_s} d^3 \, r_1 \, \varepsilon(\underline{r}_1,t) \, \underline{G}_2 \, (\underline{r}, \, \underline{r}_1) \cdot \underline{E}_2 \, (\underline{r}_1,t) \tag{21}$$

Equations (20,21) constitute integral equations which generally
cannot be solved. The simplest applicable approximation to
these equations is the so called "distorted wave Born approxima-
tion" in accordance with which one replaces $\underline{E}_2 \, (\underline{r}_1,t)$ in the
integrands of Eqs. (20,21) with $\underline{E}_2^{(0)} \, (\underline{r}_1,t)$. The quantities
$\underline{E}_2^{(0)}$ and $\underline{G}_{1,2}$ are associated with the background problem which
is discussed in the next section. It should be noted that the
validity range of the Born approximation (in absence of any
wave distorting background) has been thoroughly investigated
(e.g., ref. (2)) and further elaboration seems redundant.

13

C.    THE BACKGROUND PROBLEM (EVALUATION OF $\underset{\sim}{G}$ AND $\underline{E}^{(0)}$)

For the sake of simplicity the ground effects are presently ignored; they will, however, be added separately at the end of this section.  The problem to be considered is that of a dielectric half-space excited by an arbitrary dipole.  It is assumed for definiteness that the source is located in region 2 (the half-space $z>0$).  To obtain solutions applicable for a source situated in region 1, one simply replaces 1 by 2, 2 by 1 and z by -z.  The excitation properties of a dielectric half-space by a dipole are well understood, extensively elaborated upon in the literature and are regarded as textbook material. Despite their simplicity, no exact closed-form solutions are available and one must resort to an asymptotic description which is readily interpretable in geometric-optical terms.

1.    The Exact Solution.

The satisfaction of the equations

$$\nabla \times \underline{E}_1^{(0)} = j\omega_o\mu_o \underline{H}_1^{(0)} \qquad \nabla \times \underline{E}_2^{(0)} = -j\omega_o\mu_o \underline{H}_2^{(0)} \tag{22}$$

$$\nabla \times \underline{H}_1^{(0)} = j\omega_o\varepsilon_1 \underline{E}_1^{(0)} \qquad \nabla \times \underline{H}_2^{(0)} = j \omega_o\varepsilon_2 \underline{E}_2 + \underline{J}_2 \delta(\underline{r} - \underline{r}')$$

with the continuity conditions

$$\underline{E}_{1t}^{(0)} = \underline{E}_{2t}^{(0)}, \quad \underline{H}_{1t}^{(0)} = \underline{H}_{2t}^{(0)} \text{ at } z=0 \tag{23}$$

and the radiation condition at infinity is required.

14

The boundary value problem is conveniently describable by the vector potential

$$\underline{H}_{\frac{1}{2}} = \nabla \times \underline{A}_{\frac{1}{2}} \quad , \quad \underline{E}_{\frac{1}{2}} = -j\omega_o\mu_o \left[ \underset{\sim}{1} + \frac{\nabla \nabla}{k_{\frac{1}{2}}^2} \right] \cdot \underline{A}_{\frac{1}{2}} \tag{24}$$

with $\underline{A}_{\frac{1}{2}}$ obeying the reduced wave equation:

$$(\nabla^2 + k_1^2) \, \underline{A}_1 = 0 \tag{25}$$

$$(\nabla^2 + k_2^2) \, \underline{A}_2 = -\underline{J}_2 \, \delta(\underline{r} - \underline{r}') \tag{26}$$

Assume the following plane-wave representation.

$$\underline{A}_{\frac{1}{2}}(r) = \frac{1}{(2\pi)^2} \int d^2 k_t \, \widehat{\underline{A}}_{\frac{1}{2}} \, (\underline{k}_t, z) \, e^{-j\underline{k}_t \cdot (\underline{\rho} - \underline{\rho}')} \tag{27}$$

hence

$$\left[ \frac{d^2}{dz^2} + \varkappa_1^2 \right] \, \widehat{\underline{A}}_1 = 0 \tag{28}$$

$$\left[ \frac{d^2}{dz^2} + \varkappa_2^2 \right] \, \widehat{\underline{A}}_2 = -\underline{J}_2 \, \delta(z - z'), \quad \varkappa_{\frac{1}{2}}^2 = k_{\frac{1}{2}}^2 - k_t^2 \tag{29}$$

where, $\underline{\rho} = \underline{r} - \underline{z}_o z$ , $\underline{\rho}' = \underline{r}' - \underline{z}_o z'$ and $\underline{k}_t$ denotes the transverse wavevector.

$\widehat{\underline{A}}_{\frac{1}{2}}$ are of the form

15

$$\underline{\hat{A}}_2 = \left[ \underset{\sim}{I} \, e^{-j\varkappa_2 (z-z')} + \underset{\sim}{\Gamma} \, e^{j\varkappa_2 (z + z')} \right] \cdot \underline{A}_0 \tag{30}$$

$$\underline{\hat{A}}_1 = \underset{\sim}{T} \cdot \underline{A}_o \quad e^{-j\varkappa_1 z + j\varkappa_2 z'} \tag{31}$$

where

$$\underset{\sim}{\Gamma} = \Gamma_H \left[ \underset{\sim}{I}_t - \frac{\varkappa_2}{k_t^2} \, z_o \, \underline{k}_t \right] + \Gamma_E \left[ \underline{z}_o \underline{z}_o - \frac{\varkappa_2}{k_t^2} \, \underline{z}_o \, \underline{k}_t \right] \tag{32}$$

$$\underset{\sim}{T} = T_H \left[ \underset{\sim}{I}_t + \frac{\varkappa_1}{k_t^2} \, z_o \, \underline{k}_t \right] + T_E \left[ \underline{z}_o \, \underline{z}_o - \frac{\varkappa_2}{k_t^2} \, \underline{z}_o \, \underline{k}_t \right] \tag{33}$$

consistently with the continuity conditions at $z = 0$, and

$$\underline{A}_o = \frac{\underline{J}_2}{2j\varkappa_2} \tag{34}$$

consistently with the prescribed dipole excitation. $\underset{\sim}{I}$ represents the transverse dyadic

$$\underset{\sim}{I}_t = \underset{\sim}{I} - \underline{z}_o \, \underline{z}_o \tag{35}$$

$\Gamma_H$ ($T_H$) and $\Gamma_E$ ($T_E$) denote the reflection (transmission) coefficients associated with the H and E-mode constituents, respectively. They are given by:

$$\Gamma_H = \frac{\varkappa_2 - \varkappa_1}{\varkappa_2 + \varkappa_1} \quad , \qquad T_H = \frac{2\varkappa_2}{\varkappa_2 + \varkappa_1} \tag{36}$$

16

$$\Gamma_E = \frac{k_1^2 \,\varkappa_2 - k_2^2 \,\varkappa_1}{k_1^2 \,\varkappa_2 + k_2^2 \,\varkappa_1} \;, \qquad T_E = \frac{2k_1^2 \,\varkappa_2}{k_1^2 \,\varkappa_2 + k_2^2 \,\varkappa_1} \qquad (37)$$

It is customary, although for some purposes, inconvenient, to make a transition from the plane-wave representation (27) which involves a two-fold integration to a cylindrical representation involving a single integral. Omitting intermediate algebraic steps, one obtains:

$$\underline{A}_2(\underline{r},\,\underline{r}') = \frac{1}{8\pi j} \int_{-\infty}^{\infty} d\beta \, \frac{\beta}{\varkappa_2} \, H_0^{(2)} \, (\beta|\underline{\rho}-\underline{\rho}'|) \left[ \underline{I} \, e^{-j\varkappa_2|z-z'|} \right.$$
$$+ \underset{\sim}{\Gamma} \, (\beta) e^{j\varkappa_2(z+z')} \left] \cdot \underline{J}_2 + \frac{\underline{z}_0}{8\pi} \left[ \nabla_t \int_{-\infty}^{+\infty} d\beta \, \frac{\beta}{\varkappa_2} \, H_0^{(2)} \right.$$
$$\left. x \, (\beta|\underline{\rho}-\underline{\rho}'|) \, \Gamma_2 \, (\beta) \, e^{j\varkappa_2(z+z')} \right] \cdot \underline{J}_2 \qquad (38)$$

$$\underline{A}_1(\underline{r},\underline{r}') = \frac{1}{8\pi j} \int_{-\infty}^{+\infty} d\beta \, \frac{\beta}{\varkappa_2} \, H_0^{(2)} \, (\beta|z-z'|) \, \underset{\sim}{T}_1 \, (\beta) \, e^{-j\varkappa_1 z + j\varkappa_2 z'} \cdot \underline{J}_2$$
$$+ \frac{\underline{z}_0}{8\pi} \left[ \nabla_t \int_{-\infty}^{\infty} d\beta \, \frac{\beta}{\varkappa_2} \, H_0^{(2)} \, (\beta|\underline{\rho}-\underline{\rho}'|) \, T_2 \, (\beta) \right.$$
$$\left. x \, e^{-j\varkappa_1 z + j\varkappa_2 z'} \right] \cdot \underline{J}_2 \qquad (39)$$

where $\nabla_t = \nabla - \underline{z}_0 \frac{\partial}{\partial z}$ denotes the transverse gradient, $\beta \equiv |\underline{k}_t|$ and $\underset{\sim}{T}_1$, $\underset{\sim}{\Gamma}_1$, $T_2$ and $\Gamma_2$ are defined by the relations:

17

$$\underset{\sim}{T}_1 = T_H \underset{\sim}{I}_t + T_E \underset{\sim}{z}_o \underset{\sim}{z}_o \tag{40}$$

$$\underset{\sim}{\Gamma}_1 = \Gamma_H \underset{\sim}{I}_t + \Gamma_E \underset{\sim}{z}_o \underset{\sim}{z}_o \tag{41}$$

$$T_2 = \frac{1}{\beta^2} (\varkappa_1 T_H - \varkappa_2 T_E) \tag{42}$$

$$\Gamma_2 = - \frac{\varkappa_2}{\beta^2} (\Gamma_H + \Gamma_E) \tag{43}$$

The above quantities are related to the previously defined $\underset{\sim}{\Gamma}$ and $\underset{\sim}{T}$ via

$$\underset{\sim}{\Gamma} = \underset{\sim}{\Gamma}_1 + \Gamma_2 \underset{\sim}{z}_o \underset{\sim}{k}_t \tag{44}$$

$$\underset{\sim}{T} = \underset{\sim}{T}_1 + T_2 \underset{\sim}{z}_o \underset{\sim}{k}_t \tag{45}$$

Equations (38, 39) cannot be further reduced and as expected the resort to approximation is unavoidable.

2.      The Asymptotic Evaluation.  The Geometric-Optical Contribution.

We first replace $H_o^{(2)} (\beta|\underset{\sim}{\rho}-\underset{\sim}{\rho}'|)$ in Eqs. (38, 39) by its asymptotic values

$$H_o^{(2)}(x) \sim \sqrt{\frac{2}{\pi x}} \; e^{-jx+j\frac{\pi}{4}} \left[ 1 + 0 \left(\frac{1}{x}\right) \right]$$

resulting in

$$\underset{\sim}{A}_2 (\underset{\sim}{r}, \underset{\sim}{r}') \sim \frac{e^{j\frac{\pi}{4}}}{8\pi j} \sqrt{\frac{2}{\pi|\underset{\sim}{\rho}-\underset{\sim}{\rho}'|}} \left[ \int_{-\infty}^{+\infty} d\beta \frac{\sqrt{\beta}}{\varkappa_2} \left[ \underset{\sim}{T} \; e^{-jP_1} + \underset{\sim}{\Gamma}_1 \; e^{-jP_2} \right] \right.$$

$$\left. + \underset{\sim}{z}_o \underset{\sim}{\rho}_o \int_{-\infty}^{+\infty} d\beta \; \frac{\beta^{3/2}}{\varkappa_2} \; \Gamma_2 (\beta) \; e^{-jP_2} \right] \cdot \underset{\sim}{J}_2 \tag{46}$$

18

$$\underline{A}_1 \ (\underline{r}, \ \underline{r}') \sim \frac{e^{j\frac{\pi}{4}}}{8\pi j} \sqrt{\frac{2}{\pi|\underline{\rho}-\underline{\rho}'|}} \left[ \int\limits_{-\infty}^{+\infty} d\beta \ \frac{\sqrt{\beta}}{\varkappa_2} \ \underline{\underline{T}}_1 \ (\beta) \ e^{-jP_3} \right.$$

$$\left. + \ \underline{z}_0 \ \underline{\rho}_0 \int\limits_{-\infty}^{+\infty} d\beta \ \frac{\beta^{3/2}}{\varkappa_2} \ T_2 \ (\beta) \ e^{-jP_3} \right] \cdot \underline{J}_2 \qquad (47)$$

where,

$$P_1 \ (\beta) = \beta|\underline{\rho}-\underline{\rho}'| + \varkappa_2 \ |z-z'| \qquad (48)$$

$$P_2 \ (\beta) = \beta|\underline{\rho}-\underline{\rho}'| - \varkappa_2(z+z') \qquad (49)$$

$$P_3 \ (\beta) = \beta|\underline{\rho}-\underline{\rho}'| + \varkappa_1 \ z-\varkappa_2 z' \qquad (50)$$

and the asymptotic relation $\nabla_t \sim -j\beta\underline{\rho}_0$ $(\underline{\rho}_0 = \frac{\underline{\rho}-\underline{\rho}'}{|\underline{\rho}-\underline{\rho}'|}$ is a unit vector in the $\underline{\rho}-\underline{\rho}'$ direction) has been utilized.

The major asymptotic contributions to the $\beta$-integrals (k the large parameter) come either from the vicinity of the respective saddle-points (geometric optical contributions) or (within some restrictive spatial regions) from the appropriate branch-points (lateral waves). Situations under which lateral-wave contributions are expected to dominate the channel (see Introduction) are omitted and will be reported separately. Their relative significance, however, is discussed at the end of this Section.

a)      The Saddle-Point Contributions

Consider the integral

$$I = \int\limits_{-\infty}^{\infty} d\beta \ F(\beta) \ e^{-jP(\beta)} \qquad (51)$$

19

assuming the existence of a single first order saddle-point one
obtains

$$I_{cp} \sim \sqrt{\frac{2\pi}{|P''(\beta_s)|}} \quad f(\beta_s) \; e^{-jP(\beta_s) \; -j\frac{\pi}{4} \; sgn \; (P''(\beta_s))} \tag{52}$$

where the saddle-point, $\beta_s$ is determined by the saddle-point
condition

$$P'(\beta_s) = 0 \tag{53}$$

and the prime denotes the derivative with respect to the argument.
One can readily apply the asymptotic form (52) to Eqs. (46-47).
The results are easily interpretable in geometric-optical terms
and could alternatively be derived via a direct use of geometric-
optical arguments. These are,

$$\underline{A}^{(i)} = \frac{e^{-jk_2L_i}}{4\pi L_i} \; \underline{J}_2 \tag{54}$$

$$\underline{A}^{(r)}_{sp} = \frac{e^{-jk_2(L_i + L_r)}}{4\pi(L_i + L_r)} \left[ \underline{\Gamma}_1 \; (\beta_s) + \underline{z}_o \; \underline{\rho}_o \; \beta_s \; \Gamma_2 \; (\beta_s) \right] \; \cdot \; \underline{J}_2 \tag{55}$$

$$\underline{A}^{(t)}_{sp} = \frac{e^{-j(k_2L_i + k_1L_t)}}{4\pi \; L_i} \; \sqrt{\frac{da_o}{da}} \left[ \underline{T}_1 \; (\beta_s) + \underline{z}_o \; \underline{\rho}_o \; \beta_s \; T_2 \; (\beta_s) \right] \; \cdot \; \underline{J}_2 \tag{56}$$

The length segments $L_i$, $L_r$, and $L_t$ are shown in Figures (2, 3);
da and $da_o$ denote differential cross sections of the transmitted
ray tube at the observation point and at the interface, respectively:

$$\frac{da}{da_o} = \left( 1 + \frac{L_t}{L_i} \; \frac{k_2}{k_1} \right) \left( 1 + \frac{L_t}{L_i} \; \frac{k_2 \; \cos^2 \theta_i}{k_1 \; \cos^2 \theta_t} \right) \tag{57}$$
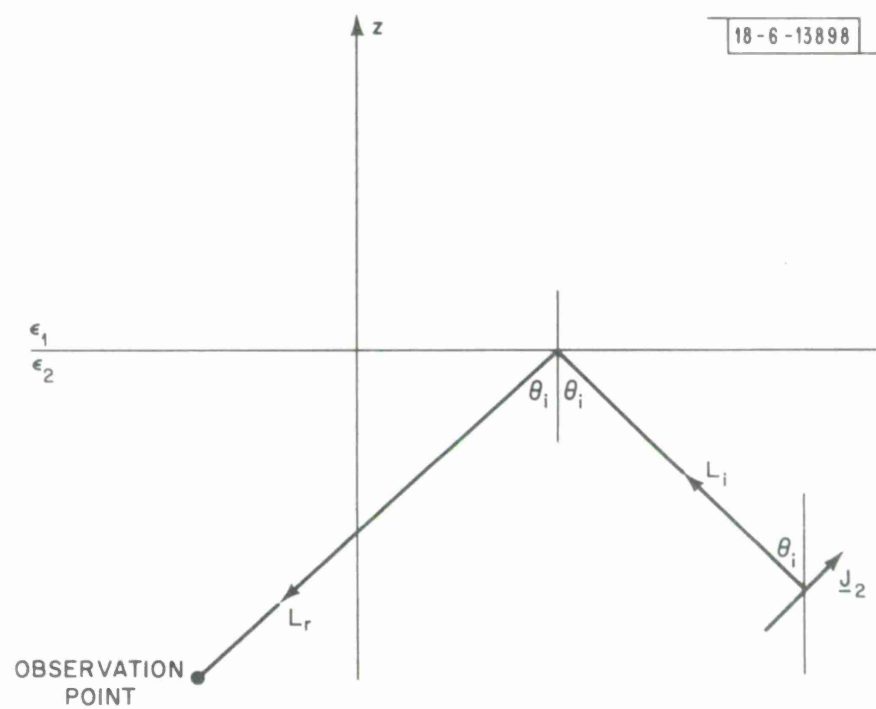
20

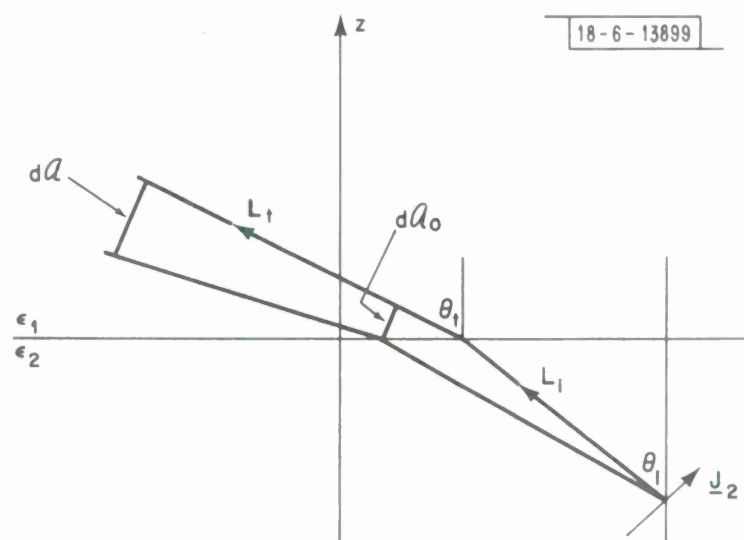Fig. 2.   The geometric - optical reflected wave.



Fig. 3.   The geometric - optical transmitted wave.

where the relationship

$$\beta_s = k_2 \sin \theta_i = k_1 \sin \theta_t \qquad (58)$$

has been used, and from Eqs. (36,37)

$$\Gamma_E (\beta_s) = \frac{k_1 \cos \theta_i - k_2 \cos \theta_t}{k_1 \cos \theta_i + k_2 \cos \theta_t}, \quad T_E (\beta_s) = \frac{2 k_1 \cos \theta_i}{k_1 \cos \theta_i + k_2 \cos \theta_t} \qquad (59)$$

$$\Gamma_H (\beta_s) = \frac{k_2 \cos \theta_i - k_1 \cos \theta_t}{k_2 \cos \theta_i + k_1 \cos \theta_t}, \quad T_H(\beta_s) = \frac{2 k_2 \cos \theta_i}{k_2 \cos \theta_i + k_1 \cos \theta_t} \qquad (60)$$

The geometric-optical electric-field is derived via Eq. (24). Neglecting rapidly decaying field constituents one obtains the incident electric field.

$$\underline{E}_{sp}^{(i)} \sim -j\omega_o \mu_o \frac{e^{-jk_2 L_i}}{4\pi L_i} (\underset{\sim}{I} - \underline{r}_o \underline{r}_o) \cdot \underline{J}_2 \qquad (61)$$

where

$$\nabla \sim -j\nabla P_1 (\beta_s) = -jk_2 \underline{r}_o, \quad \underline{r}_o \equiv \frac{\underline{r} - \underline{r}'}{|\underline{r} - \underline{r}'|} \qquad (62)$$

the reflected electric-field,

$$\underline{E}_{sp}^{(r)} \sim -j\omega_o \mu_o \frac{e^{-jk_2 (L_i + L_r)}}{4\pi (L_i + L_r)} (\underset{\sim}{I} - \widehat{\underline{r}}\widehat{\underline{r}}_o) \cdot \widehat{\underline{\Gamma}} (\beta_s) \cdot \underline{J}_2 \qquad (63)$$

where

$$\nabla \sim j\nabla P_2 (\beta_s) = -jk_2 \widehat{\underline{r}}_o, \quad \widehat{\underline{r}}_o = \frac{\underline{\rho} - \underline{\rho}' + \underline{z}_o (z + z')}{|\underline{\rho} - \underline{\rho}' + \underline{z}_o (z + z')|} \qquad (64)$$

22

$$\widehat{\underset{\sim}{\Gamma}} (\beta_s) = \Gamma_H (\beta_s) \, \underset{\sim}{I}_t + \Gamma_E (\beta_s) \, \underline{z}_o \underline{z}_o - \frac{\varkappa_2 (\beta_s)}{\beta_s}$$

$$\times \left[ \Gamma_H (\beta_s) + \Gamma_E (\beta_s) \right] \, \underline{z}_o \underline{\rho}_o \tag{65}$$

and finally the transmitted electric field,

$$\underline{E}_{sp}^{(t)} \sim -j\omega_o \mu_o \; \frac{e^{-j \, (k_2 L_i + k_1 L_t)}}{4\pi \, L_i} \; \sqrt{\frac{da_o}{da}} \; (1 - \overline{\underline{r}}_o \overline{\underline{r}}_o) \cdot \widehat{\underset{\sim}{T}}(\beta_s) \cdot \underline{J}_2 \tag{66}$$

where

$$\nabla \sim -j \nabla P_3 (\beta_s) = -jk_1 \overline{\underline{r}}_o, \quad \overline{\underline{r}}_o = \underline{\rho}_o \sin \theta_t + \underline{z}_o \cos \theta_t \tag{67}$$

and

$$\widehat{\underset{\sim}{T}} (\beta_s) = T_H (\beta_s) \, \underset{\sim}{I}_t + T_E (\beta_s) \, \underline{z}_o \underline{z}_o$$

$$+ \frac{1}{\beta_s} \left[ \varkappa_1 (\beta_s) \, T_H (\beta_s) - \varkappa_2 (\beta_s) \, T_E (\beta_s) \right] \, \underline{z}_o \underline{\rho}_o \tag{68}$$

$\underline{r}_o$, $\widehat{\underline{r}}_o$ and $\overline{\underline{r}}_o$ geometrically represent unit vectors along the incident, reflected and refracted rays. The dyadics $\underset{\sim}{1} - \underline{r}_o \underline{r}_o$, $\underset{\sim}{1} - \widehat{\underline{r}}_o \widehat{\underline{r}}_o$ and $\underset{\sim}{1} - \overline{\underline{r}}_o \overline{\underline{r}}_o$, represent transverse-projection operators with respect to the corresponding rays.

With the geometric-optical properties of the refracted wave (66) available, the desired information concerning both the incident wave and the dyadic Green's function is readily deduced. For reasons of convenience, notational changes are introduced as indicated in Figs. (4, 5). The geometric-optical Green's function
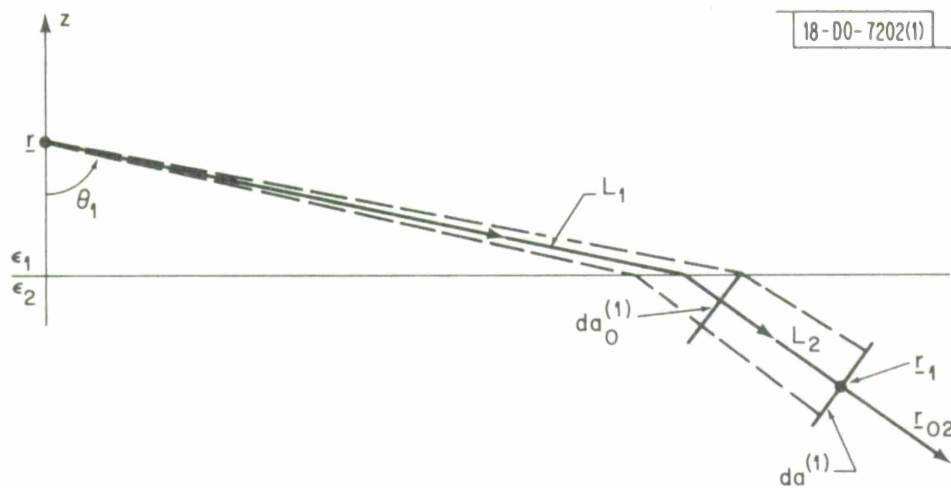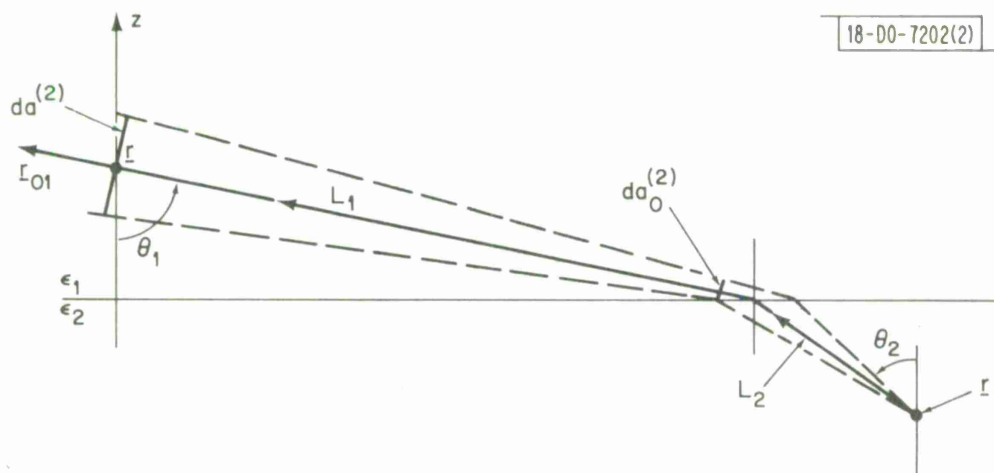
23

Fig. 4.  Incident wave.



Fig. 5.  Green's function.

24

and the incident wave (excited by an arbitrary dipole) are given by:

$$\underline{\underline{G}}_1 (\underline{r},\underline{r}_1) \sim \frac{e^{-j\,(k_1 L_1 + k_2 L_2)}}{4\pi\,L_2} \sqrt{\frac{da_o^{(2)}}{da^{(2)}}}\ (\underline{\underline{I}}_t - \underline{r}_{o1}\underline{r}_{o1})\ \cdot\ \underline{\underline{T}}_{12} \qquad (69)$$

$$\underline{E}^{(o)} (\underline{r}_1) \sim -j\omega_o\mu_o\,\frac{e^{-j\,(k_1 L_1 + k_2 L_2)}}{4\pi\,L_1} \sqrt{\frac{da_o^{(1)}}{da^{(1)}}}\ (\underline{\underline{I}}_t - \underline{r}_{o2}\underline{r}_{o2})$$

$$\cdot\ \underline{\underline{T}}_{21}\ \cdot\ \underline{J}_1 \qquad\qquad\qquad (70)$$

where

$$\underline{\underline{T}}_{12} = \left[ T_H^{(12)}\ \underline{\underline{I}}_t + T_E^{(12)}\ \underline{z}_o\underline{z}_o + \frac{\varkappa_1\,T_H^{(12)}\ -\ \varkappa_2\,T_E^{(12)}}{\beta}\ \underline{z}_o\underline{\rho}_o \right]_{\beta=\beta_s} \qquad (71)$$

$$\underline{\underline{T}}_{21} = \left[ T_H^{(21)}\ \underline{\underline{I}}_t + T_E^{(21)}\ \underline{z}_o\underline{z}_o - \frac{\varkappa_2\,T_H^{(21)}\ -\ \varkappa_1\,T_E^{(21)}}{\beta}\ \underline{z}_o\underline{\rho}_o \right]_{\beta=\beta_s} \qquad (72)$$

and

$$T_H^{(12,21)} = \frac{2\varkappa_{2,1}}{\varkappa_1 + \varkappa_2}\ ,\quad T_E^{(12,21)} = \frac{2k_{1,2}^2\,\varkappa_{2,1}}{k_1^2\,\varkappa_2 + k_2^2\,\varkappa_1} \qquad (73)$$

The radius vectors $\underline{r}$ and $\underline{r}_1$ denote the location of the source (generating the incident wave) and the scattering point, respectively. The ray-tube cross section ratios are now given by:

$$\frac{da^{(1,2)}}{da_o^{(1,2)}} = \left( 1 + \frac{L_{2,1}}{L_{1,2}}\ \frac{k_{1,2}}{k_{2,1}} \right) \left( 1 + \frac{L_{2,1}}{L_{1,2}}\ \frac{k_{1,2}}{k_{2,1}}\ \frac{\cos^2\theta_{1,2}}{\cos^2\theta_{2,1}} \right) \qquad (74)$$

Further simplifying features which stem from the presumed smallness of the angle $\delta = \frac{\pi}{2} - \theta_1$, are discussed below.

25

Specifically, the validity of the inequality

$$\sin^2 \delta \approx \delta^2 \ll 1 - \eta^{-2} \ll 1 \tag{75}$$

is assumed. Here, $\eta = k_2/k_1$ denotes the index of refraction of the half-space $z < 0$. (Typically, $\eta \approx 1.05$ and (75) becomes $\delta \ll 0.3$ radians $\approx 17^{\underline{o}}$, often a reasonable restriction for ground radars). Under the restriction (75) one may readily verify that

$$\frac{\cos^2 \theta_2}{\cos^2 \theta_1} = \frac{1 - \eta^{-2} \cos^2 \delta}{\sin^2 \delta} \approx \frac{1 - \eta^{-2}}{\sin^2 \delta} \gg 1 \tag{76}$$

consequently, the area-mappings (74) simplify to:

$$\frac{da^{(1)}}{da_o^{(1)}} \approx 1 + \frac{L_2}{L_1} \frac{k_1}{k_2} \approx 1 \tag{77}$$

$$\frac{da^{(2)}}{da_o^{(2)}} \approx \frac{L_1}{L_2} \frac{k_2}{k_1} \frac{\cos^2 \theta_2}{\cos^2 \theta_1} \left(1 + \frac{L_1}{L_2} \frac{k_2}{k_1}\right) \approx \left(\frac{L_1}{L_2} \frac{k_2}{k_1} \frac{\cos \theta_2}{\cos \theta_1}\right)^2 \tag{78}$$

where the last of the approximate forms in Eqs. (77,78) presumed the largeness of $L_1$ with respect to $L_2$. More caution must be exercised in approximating the phase function:

$$P \equiv k_1 L_1 + k_2 L_2 \tag{79}$$

The following geometrical identities hold:

$$|\underline{\rho} - \underline{\rho}_1| = L_1 \sin \theta_1 + L_2 \sin \theta_2 , \quad \underline{\rho} = \underline{r} - z\underline{z}_o, \quad \rho_1 = \underline{r}_1 - z_1 \underline{z}_o \tag{80}$$

26

$$z = L_1 \cos \theta_1 \qquad (81)$$

$$-z_1 = L_2 \cos \theta_2 \qquad (82)$$

From Eq. (76) it follows that $\dfrac{d\theta_2}{d\theta_1} = \dfrac{k_1 \cos \theta_1}{k_2 \cos \theta_2} \ll 1$, hence, for large $|\rho-\rho_1|$ (small $\delta$) the angle $\theta_2$ stays virtually constant approaching the critical angle of refraction:

$$\sin \theta_2 \approx \frac{k_1}{k_2} = \frac{1}{\eta} \qquad (83)$$

It follows that:

$$L_2 \approx \frac{-z_1}{\sqrt{1 - \eta^{-2}}} \qquad (84)$$

To determine $L_1$ we substitute Eq. (81) into (80) resulting in

$$|\rho-\rho_1| = (L_1 + L_2 \frac{k_1}{k_2}) \sin \theta_1 = (L_1 + L_2 \frac{k_1}{k_2}) \left[1 - (\frac{z}{L_1})^2\right]^{1/2} \qquad (85)$$

upon expansion of the square root one obtains

$$k_1 L_1 \approx k_1 |\rho-\rho_1| \left[1 + \frac{1}{2} \left(\frac{z}{L_1}\right)^2 + \frac{3}{8} \left(\frac{z}{L_1}\right) + \ldots\right] - \frac{k_1^2}{k_2} L_2 \qquad (86)$$

Neglegence of the fourth power contribution to the phase function is justified subject to the constraint

$$k_1 |\rho-\rho_1| \left(\frac{z}{L_1}\right)^4 \ll 1 \qquad (87)$$

which is an acceptable assumption under the prevailing circumstances. (Typically, at UHF: $k_1 |\rho-\rho_1| (\frac{z}{L_1})^4 < 0 \ (10^{-3})$ .

27

From Eqs. (85,87) it follows that

$$|\underline{\rho}-\underline{\rho}_1| \approx (L_1 + \frac{1}{\eta} L_2) \left[1 - \frac{1}{2}\left(\frac{z}{L_1}\right)^2\right]^2 = L_1 - \frac{1}{2} \frac{z^2}{L_1}$$

$$+ \frac{1}{\eta} L_2 - \frac{1}{2\eta} L_2 \left(\frac{z}{L_1}\right)^2 \tag{88}$$

and presuming

$$\frac{1}{2} k_2 L_2 \left(\frac{z}{L_1}\right)^2 \ll 1 \tag{89}$$

(once again a reasonable assumption under typical conditions at UHF:

$$\frac{1}{2} k_2 L_2 \left(\frac{z}{L_1}\right)^2 \lesssim 0 \ (10^{-2})$$ one readily solves the resulting

quadratic equation for $L_1$:

$$L_1 \approx \frac{1}{2} \left(|\underline{\rho}-\underline{\rho}_1| - \frac{L_2}{\eta}\right) \left[1 + \sqrt{1 + \frac{2z^2}{\left[|\underline{\rho}-\underline{\rho}_1| - \frac{L_2}{\eta}\right]^2}}\right] \approx$$

$$\left(|\underline{\rho}-\underline{\rho}_1| - \frac{L_2}{\eta}\right) \left[1 + \frac{z^2}{2\left[|\underline{\rho}-\underline{\rho}_1| - \frac{L_2}{\eta}\right]^2}\right] \tag{90}$$

The square-root expansion in (90) brings about a constraint already imposed by (87).

We finally have

$$L_1 = |\underline{\rho}-\underline{\rho}| - \frac{L_2}{\eta} + \frac{1}{2} \frac{z^2}{|\underline{\rho}-\underline{\rho}_1| + \frac{L_2}{\eta}} \approx |\underline{\rho}-\underline{\rho}_1| - \frac{L_2}{\eta}$$

$$+ \frac{1}{2} \frac{z^2}{|\underline{\rho}-\underline{\rho}_1|} \tag{91}$$

The last form presumes the smallness of the term $\frac{1}{2} k_1 \frac{z^2 L_2}{|\underline{\rho}-\underline{\rho}_1|^2}$

a restriction equivalent to (89). The phase function is given by:

$$P \approx k_1 \left[ |\underline{\rho}-\underline{\rho}_1| + \frac{1}{2} \frac{z^2}{|\underline{\rho}-\underline{\rho}_1|} \right] - k_2 \sqrt{1 - \eta^{-2}} \, z_1 \tag{92}$$

The last result is simply interpretable as illustrated in Fig. 6.
Equation (79) may be rewritten as:

$$P = k_1 \sqrt{|\underline{\rho}-\underline{\rho}_1|^2 + z^2} + k_1 \left[ L_1 - \sqrt{|\underline{\rho}-\underline{\rho}_1|^2 + z^2} \right] + k_2 L_2 \tag{93}$$

The approximation (92) amounts to replacing the bracketed term
by $-L_2 \sin \theta_2$ (see Fig. 6) and to the subsequent expansion of
the square root, retaining the two leading terms. Equation (92)
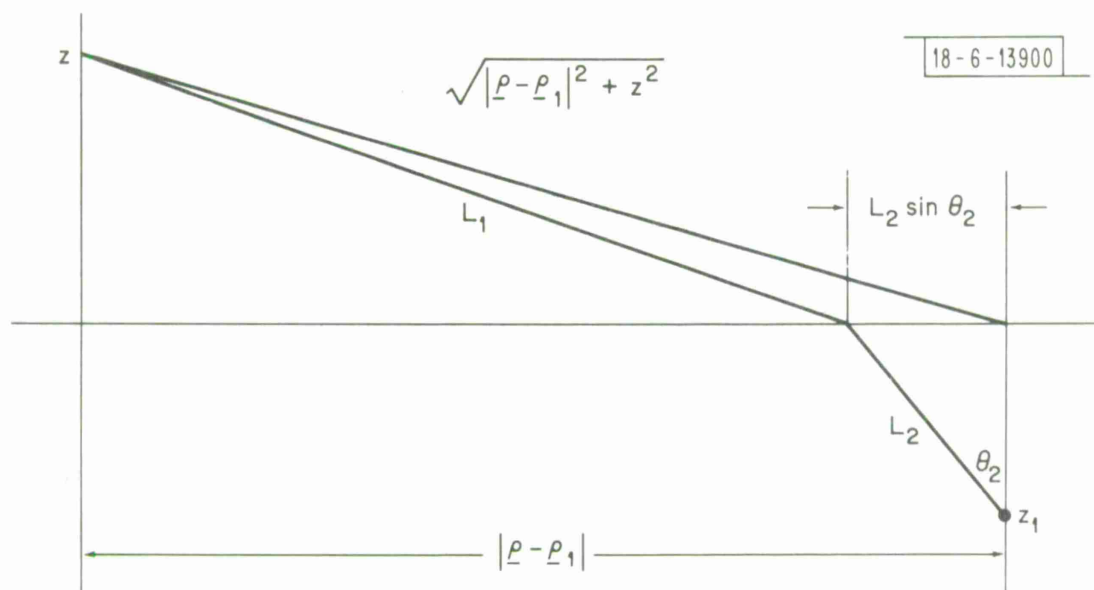follows directly.

29

Fig. 6.   Interpretation of the phase function.

The polarization properties of the incident wave and the Green's functions are determined by the operators $(\underset{\sim}{1} - \underline{r}_{o2}\underline{r}_{o2}) \cdot \underset{\sim}{T}_{21}$ and $(\underset{\sim}{1} - \underline{r}_{o1}\underline{r}_{o1}) \cdot \underset{\sim}{T}_{12}$ (see Eqs. (69-72)), respectively. These operators simplify substantially in view of (75). One has,

$$
\begin{aligned}
(\underset{\sim}{1}-\underline{r}_{o1}\underline{r}_{o1}) \cdot \underset{\sim}{T}_{12} &= \Big[\underset{\sim}{1} - \underline{\rho}_{o}\underline{\rho}_{o} \sin^2 \theta_1 - \underline{z}_{o}\underline{z}_{o} \cos^2 \theta_1 \; (\underline{\rho}_{o}\underline{z}_{o} + \underline{z}_{o}\underline{\rho}_{o}) \\
&\quad \sin \theta_1 \cos \theta_1 \Big] \cdot \underset{\sim}{T}_{12} \approx \Big[\underset{\sim}{1} - \underline{\rho}_{o}\underline{\rho}_{o}\Big] \cdot \underset{\sim}{T}_{12} \approx T_H^{(12)} \; (\underset{\sim}{1}_t - \underline{\rho}_{o}\underline{\rho}_{o}) \\
&\quad + T_E^{(12)} \Big[\underline{z}_{o}\underline{z}_{o} - \underline{z}_{o}\underline{\rho}_{o} \cot \theta_2 \Big]
\end{aligned}
\tag{94}
$$

where terms of order $\cos \theta_1 = \sin \delta \approx \delta$ have been omitted. The depolarization may also be neglected owing to the smallness of

$$
\cot \theta_2 \approx \sqrt{\eta^2 - 1} \ll 1
$$

Similarly,

$$
\begin{aligned}
(\underset{\sim}{1} - \underline{r}_{o2}\underline{r}_{o2}) \cdot \underset{\sim}{T}_{21} &= \Big[\underset{\sim}{1} - \underline{\rho}_{o}\underline{\rho}_{o} \sin^2\theta_2 - \underline{z}_{o}\underline{z}_{o} \cos^2\theta_2 - (\underline{\rho}_{o}\underline{z}_{o} + \underline{z}_{o}\underline{\rho}_{o}) \\
&\quad \sin \theta_2 \cos \theta_2 \Big] \cdot \underset{\sim}{T}_{21} \approx T_H^{(21)} \; (\underset{\sim}{1}_t - \underline{\rho}_{o}\underline{\rho}_{o}) \\
&\quad + T_E^{(21)} \; \underline{z}_{o}\underline{z}_{o}
\end{aligned}
\tag{95}
$$

where once again the smallness of the parameters $\delta$ and $1-\eta^2$ was presumed. With restriction (76) borne in mind, the following simplified forms of the transmission coefficients results:

$$
T_H^{(12)} \approx T_E^{(12)} \approx 2
\tag{96}
$$

31

$$T_H^{(21)} \approx \frac{1}{\eta^2} \quad T_E^{(21)} \approx \frac{2}{\eta} \frac{\cos\theta_1}{\cos\theta_2} = \frac{2}{\sqrt{\eta^2-1}} \frac{z}{L_1} \tag{97}$$

The substitution of Eqs. (77,78,92,96,97) into Eqs. (69,70), results in the following simplified geometric-optical expressions:

$$\underline{G}_1(\underline{r},\underline{r}_1) \sim \frac{z[\underline{1} - \underline{\rho}_0\underline{\rho}_0]}{2\pi\sqrt{\eta^2-1}\ L_1^2} \quad e^{-jk_1\left[|\underline{\rho} - \underline{\rho}_1| + \frac{1}{2}\frac{z^2}{|\underline{\rho}-\underline{\rho}_1|}\right.}$$

$$\left. - \sqrt{\eta^2-1}\ z_1\right] \ -\alpha L_2 \tag{98}$$

and

$$\underline{E}^{(o)}(\underline{r}_1) \sim -j\omega_0\mu_0 \ \frac{z[\underline{1} - \underline{\rho}_0\underline{\rho}_0]\cdot\underline{J}_1}{2\pi\sqrt{\eta^2-1}\ L_1^2} \quad e^{-jk_1\left[|\underline{\rho}-\underline{\rho}_1|\right.}$$

$$\left. + \frac{1}{2}\frac{z^2}{|\underline{\rho}-\underline{\rho}_1|} - \sqrt{\eta^2-1}\ z_1\right] \ -\alpha L_2 \tag{99}$$

where a decay term exp $(-\alpha L_2)$ has been written explicitly (not as the imaginary part of $k_2$), and $L_{1,2}$ are given by Eqs. (84,91). (The last two terms in Eq. (91) may be totally ignored in the amplitude factor of Eq. (99).)

For a horizontal dipole, we have

$$(\underline{1} - \underline{\rho}_0\underline{\rho}_0)\cdot\underline{J}_1 = \underline{\varphi}_0\underline{\varphi}_0\cdot\underline{J}_1 = \underline{\varphi}_0 J_{1\varphi} = \underline{\varphi}_0 J_1 \cos\varphi \tag{100}$$

(see Fig. 7)

The incident field may be further generalized if one cares to account for the finite aperture of the antenna. Equation (99)

32

Fig. 7.   Top view.

may be rewritten as:

$$\underline{E}^{(o)}(\underline{r}_1) \sim F(\varphi) \frac{2z}{\sqrt{\eta^2-1}\, L_1^2}\; e^{-jk_1\left[|\underline{\rho}-\underline{\rho}_1| + \frac{1}{2}\frac{z^2}{|\underline{\rho}-\underline{\rho}_1|} -\sqrt{\eta^2-1}\, z_1\right] -\alpha L_2}\underline{\varphi}_o$$

(101)

where $F(\varphi)$ is simply related to the incident field as follows:

$$F(\varphi) = F(\theta,\varphi)_{\theta=0} \tag{102}$$

$$\underline{E}^{(i)} \sim F(\theta,\varphi)\frac{e^{-jk_1 L_1}}{L_1}\underline{\varphi}_o \tag{103}$$

From basic definition of the antenna gain (ignoring medium effects) via,

$$g(\theta,\varphi) \equiv \frac{4\pi L_1^2\, S_r^{(i)}}{P_t} = 2\pi\sqrt{\frac{\epsilon_o}{\mu_o}}\;\frac{|F(\theta,\varphi)|^2}{P_t} \tag{104}$$

It follows from Eqs. (102, 103, 104) that

$$|F(\varphi)|^2 \approx \frac{1}{2\pi}\;\sqrt{\frac{\mu_o}{\epsilon_o}}\; P_t[g(\theta,\varphi)]_{\theta=0} \tag{105}$$

where $P_t$ denotes the total power emitted from the antenna. It should be recalled that the antenna's finite aperture not only plays a role by controlling the incident radiation, but also by receiving the backscattered signal. The necessary related modifications are described in the next section.

b.    Ground Effects

The presence of the ground, so far totally ignored, can be accounted for without difficulty. For the horizontally polarized component the ground could, quite accurately, be modeled as a perfectly reflecting surface. Furthermore, multiple reflections between the two interfaces may, safely, be neglected owing to the lossy character of the vegetation slab. A single ground reflection of either the incident wave or the Green's function (or both) is expected to constitute an adequate description of the phenomenon. Geometric-optical contributions to be dealt with are illustrated in Figs. (8a and 8b). The ground reflected constituents may be written by inspection from Eqs. (98,99, or 101) by a proper phase inversion (for horizontal polarization) and by replacing $-z_1$ with $2h + z_1$. We have,
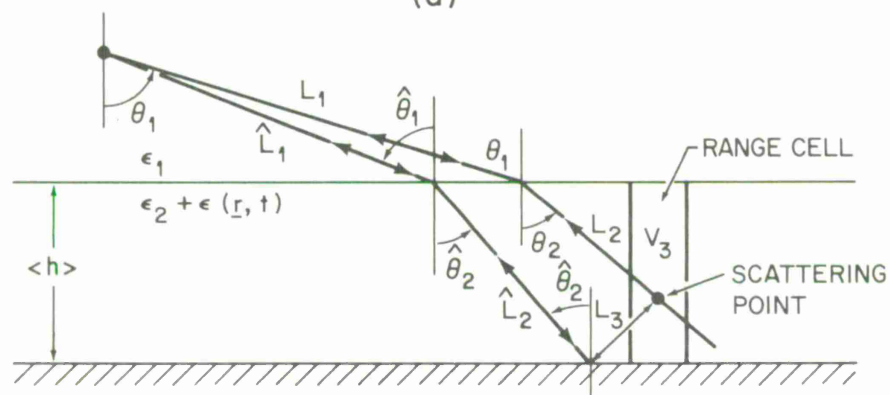
$$\underset{\sim}{G}_{1R}(\underline{r},\underline{r}_1) \sim -\frac{z(1_t - \underline{\rho}_o\underline{\rho}_o)}{2\pi\sqrt{\eta^2-1}\ L_1^2}\ e^{-jk_1\left[|\underline{\rho}-\underline{\rho}_1| + \frac{z^2}{|\underline{\rho}-\underline{\rho}_1|} + \sqrt{\eta^2-1}\ (2h + z_1)\right]} - \frac{\alpha(2h + z_1)}{\sqrt{1 - \eta^{-2}}}$$

(106)

(Note:  the $\underline{z}_o\underline{z}_o$ element does not experience a phase reversal but it plays no significant role in future calculations.) Similarly,

35

18-D0-7203(1)
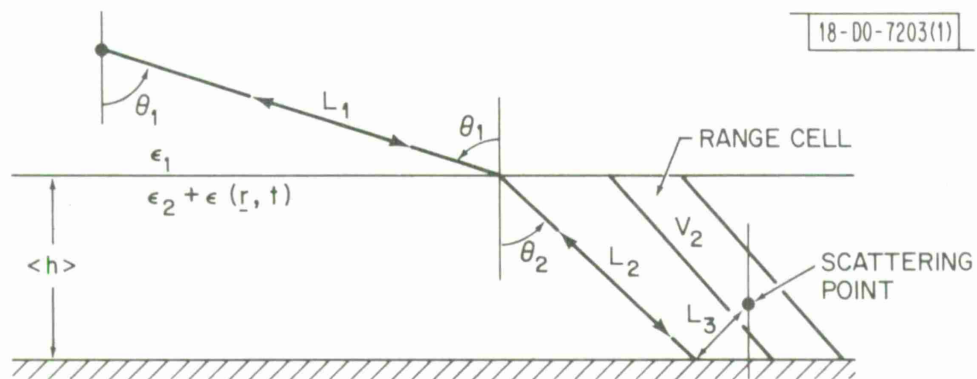
Fig. 8. Geometric - optical contributions.

36

$$E_R^{(o)}(\underline{r}_1) \sim - \underline{\varphi}_o \, F(\varphi) \, \frac{2z}{\sqrt{\eta^2-1} \, L_1^2} \, e^{-jk_1 \left[ |\underline{\rho}-\underline{\rho}_1| + \frac{1}{2} \frac{z^2}{|\underline{\rho}-\underline{\rho}_1|} \right.}$$

$$\left. + \sqrt{\eta^2-1} \, (2h + z_1) \right] - \frac{\alpha(2h + z_1)}{\sqrt{1-\eta^{-2}}} \qquad (107)$$

c.      Comparison with the Lateral Wave Contribution

Under certain conditions the geometric-optical field (Eqs. (98,99)) does not represent an adequate description of the incident radiation or the Green function. Specifically, as the radiating source or the point of observation approach the interface, i.e., as $z \to 0$, the geometric-optical field vanishes and clearly, it no longer constitutes the major filed contribution. Whenever the transmitting and/or receiving antennas are situated in the proximity of or below the (air-vegetation) interface, it is a diffracted contribution, the lateral wave, which dominates. While work has been done to account for such situations, its report is deferred for the future. Under the conditions stated in (75) the dipole-excited lateral wave is given approximately by:

37

$$\left|\underline{E}_L^{(o)}\right| \sim \frac{\omega_o\,\mu_o}{2\pi k_1(\eta^2-1)} \quad \frac{}{\sqrt{\left|\underline{\rho}-\underline{\rho}_1\right|}\ L_L^{3/2}} \tag{108}$$

where $L_L$ denotes the lateral path. Consequently, comparison with eq. (99) yields,

$$\frac{\left|\underline{E}_L^{(o)}\right|}{\left|\underline{E}^{(o)}\right|} \sim \frac{1}{k_1\,z\sqrt{\eta^2-1}} = \frac{1}{2\pi\sqrt{\eta^2-1}}\ \frac{\lambda}{z} \tag{109*}$$

Typically, for antennas situated several wavelengths above the vegetation air interface, the lateral-wave may be safely neglected.

D. THE DISTORTED WAVE BORN APPROXIMATION. THE RECEIVED CLUTTER POWER (MEAN AND VARIANCE)

The title "Distorted Wave Born" generally refers to a class of single-scattering approximations in which the propagation features of both the incident wave (on the way to the scattering volume) as well as the scattered wave (on its way to the receiver) are modified consistently with a suitably defined background (in our case a lossy, uniform dielectric slab). In the following analysis we refrain from generalizing any of the results beyond restrictions applicable for the specific configuration. Several such generalizations however are within easy reach. From eq. (21) together with (98, 101) one readily obtains:

---

* Similar observations were made by T. Tamir in an ECOM Memorandum (Summer 1970) entitled, "The Electromagnetic Field Radiated Above a Forest by an Antenna Embedded in Vegetation".

$$\underline{E}_{ls}(\underline{r}, t) = \frac{\omega_o^2 \mu_o z^2}{\pi(\eta^2 - 1)\rho_o^4} \int_{V_s} d^3 r_1 \underline{\varphi}_o F(\varphi)\, \epsilon(\underline{r}_1, t)$$

$$e^{-j2k_1\left[\,|\underline{\rho} - \underline{\rho}_1| + \frac{1}{2} \frac{z^2}{|\underline{\rho} - \underline{\rho}_1|} - \sqrt{\eta^2 - 1}\; z_1\,\right] + \frac{2\alpha z_1}{\sqrt{1 - \eta^{-2}}}} \qquad (110)$$

where $L_1$ has been replaced by $\rho_o$ in the amplitude term (see eq. 91 and Fig. 7).

Let us focus our attention on the scattering contributions from a volume $\Delta V_i$ (Fig. 7) such that $\rho_o \Delta\varphi_i$ is large compared to the transverse correlation distance (but small enough to obey restrictions (113, 114). We have,

$$\Delta \underline{E}_{si}(\underline{r}, t) \sim \frac{\omega_o^2 \mu_o z^2}{\pi(\eta^2 - 1)\rho_o^4} \int_{\Delta V_i} d^3 r_1 \underline{\varphi}_o F(\varphi)\, \epsilon(\underline{\rho}_i + \underline{r}_1, t)$$

$$e^{-j2k_1\left[\,|\underline{\rho} - \underline{\rho}_i - \underline{\rho}_1| + \frac{1}{2} \frac{z^2}{|\underline{\rho} - \underline{\rho}_i - \underline{\rho}_1|} - \sqrt{\eta^2 - 1}\; z_1\,\right] + \frac{2\alpha z_1}{\sqrt{1 - \eta^{-2}}}} \qquad (111)$$

The Taylor expansion

$$|\underline{\rho} - \underline{\rho}_i - \underline{\rho}_1| \approx \rho_o - \underline{\rho}_{oi} \cdot \underline{\rho}_1 + \frac{1}{2\rho_o}\left[\underline{\rho}_1^2 - (\underline{\rho}_{oi} \cdot \underline{\rho}_1)^2\right] + \ldots,$$

$$|\underline{\rho} - \underline{\rho}_i| = \rho_o, \quad \underline{\rho}_{oi} = \frac{\underline{\rho} - \underline{\rho}_i}{\rho_o} \qquad (112)$$

together with the assumptions

$$k_1 \frac{\rho_{1\,max}^2}{\rho_o} \ll 1, \quad \rho_{1\,max} = \max\left\{d \text{ or } \rho_o \Delta\varphi_i\right\} \qquad (113)$$

$$k_1 \rho_{1\,max}\left(\frac{z}{\rho_o}\right)^2 \ll 1 \qquad (114)$$

39

result in,

$$\Delta \underline{E}_{si}(\underline{r}, t) \sim \frac{\omega_o^2 \mu_o z^2}{\pi (\eta^2 - 1) \rho_o^4} \, e^{-jk_1 \frac{z^2}{\rho_o} -j2k_1\rho_o} F(\varphi_i) \, \underline{\varphi}_{oi}$$

$$\int_{\Delta V_i} d^3 r_1 \, \epsilon(\underline{\rho}_i + \underline{r}_{1'}, t) \, e^{j2k_1\underline{\rho}_{oi} \cdot \underline{\rho}_1 + j2k_1 \sqrt{\eta^2 - 1} \, z_1 + \frac{2\alpha z_1}{\sqrt{1 - \eta^{-2}}}} \tag{115}$$

where it has been furthermore assumed that $\underline{\varphi}_o$ and $F(\varphi)$ stay virtually constant over the volume of integration $(\Delta V_i)$.

Before proceeding with the analysis let us generalize eqs. (110 and 115) to include the ground effects. We have (via eq. 20),

$$\underline{E}_{1s}(\underline{r}, t) \sim \omega_o^2 \mu_o \int_{V_s} d^3 r_1 \, \epsilon(\underline{r}_1, t) \, (\underline{\underline{G}}_1(\underline{r}, \underline{r}_1) + \underline{\underline{G}}_{1R}(\underline{r}, \underline{r}_1)) \cdot (\underline{E}^{(o)}(\underline{r}_1) + \underline{E}_R^{(o)}(\underline{r}_1))$$

$$\tag{116}$$

where $\underline{\underline{G}}_1$, $\underline{\underline{G}}_{1R}$, $\underline{E}^{(o)}$ and $\underline{E}_R^{(o)}$ are given in eqs. (98, 101, 106 and 107).

Explicitly:

$$\underline{E}_{1s}(\underline{r}, t) \sim \frac{\omega_o^2 \mu_o z^2}{\pi (\eta^2 - 1)\rho_o^4} \int_{V_s} d^3 r_1 \, \underline{\varphi}_o F(\varphi) \, \epsilon(\underline{r}_1, t) \left[ 1 - e^{\left[ -j2k_1 \sqrt{\eta^2-1} - \frac{2\alpha}{\sqrt{1-\eta^{-2}}} \right] (h+z_1)} \right]^2$$

$$e^{-j2k_1 \left[ |\underline{\rho} - \underline{\rho}_1| + \frac{1}{2} \frac{z^2}{|\underline{\rho} - \underline{\rho}_1|} - \sqrt{\eta^2 - 1} \, z_1 \right] + \frac{2\alpha z_1}{\sqrt{1 - \eta^{-2}}}} \tag{117}$$

The effects of the perfectly conducting ground are totally contained in the bracketed term (to be denoted $\gamma(z_1)$) its replacement by unity leads back to eq. (110). Analogously to eq. (115) one now has,

$$\Delta \underline{E}_{si}(\underline{r}, t) \sim \frac{\omega_o^2 \mu_o z^2}{\pi (\eta^2 - 1) \rho_o^4} e^{-jk_1 \frac{z^2}{\rho_o}} -j2k_1\rho_o F(\varphi_i) \underline{\varphi}_{oi}$$

$$\int\limits_{\Delta V_i} d^3 r_1 \, \epsilon(\underline{\rho}_i + \underline{r}_1, t) \, \gamma(z_1) \, e^{j2k_1 \underline{\rho}_{oi} \cdot \underline{\rho}_1 + 2jk_1 \sqrt{\eta^2 - 1} z_1 + \frac{2 \alpha z_1}{\sqrt{1 - \eta^{-2}}}} \tag{118}$$

It is important to point out an error introduced in writing eq. (116). The scattering volume $V_s$ is determined (longitudinally) by the radar's gating. In eq. (116) we identify four distinct and readily interpretable terms, each associated with a somewhat different range cell. The forms (116-118) totally ignore such differences.

Since the volume $\Delta V_i$ has been selected consistently with the requirement that $\rho_o \Delta \varphi_i$ be large with respect to the correlation length, it follows that the scattering volume $\Delta V_i$ and $\Delta V_j$ ($j \neq i$) are uncorrelated, hence

$$< \Delta \underline{E}_{si} \cdot \Delta \underline{E}_{sj}^* > = < |\Delta \underline{E}_{si}|^2 > \delta_{ij} \tag{119}$$

where $< >$ denotes ensemble averaging. We now compute the field's temporal correlation from eq. (118)

$$< \Delta \underline{E}_{si}(\underline{r}, t) \cdot \Delta \underline{E}_{si}^*(\underline{r}, t+\tau)> = \frac{\omega_o^4 \mu_o^2 z^4}{\pi^2 (\eta^2 - 1)^2 \rho_o^8} |F(\varphi_i)|^2 \int\limits_{\Delta V_i} d^3 r_1 \int\limits_{\Delta V_i} d^3 r_2 \, \gamma(z_1) \, \gamma^*(z_2)$$

$$C(\underline{r}_1, \underline{r}_2, \tau) \, e^{j2k_1 \underline{\rho}_{oi} \cdot (\underline{\rho}_1 - \underline{\rho}_2) + j2k_1 \sqrt{\eta^2 - 1} (z_1 - z_2) + \frac{2 \alpha (z_1 + z_2)}{\sqrt{1 - \eta^{-2}}}} \tag{120}$$

where,

$$C(\underline{r}_1, \underline{r}_2, \tau) \equiv < \epsilon(\underline{r}_1, t) \, \epsilon^*(\underline{r}_2, t + \tau) > \tag{121}$$

is the space-time correlation of the presumedly stationary random process $\epsilon$.

41

It is convenient to separate the vertical from the horizontal coordinates in eq. (120) and transform to the center of mass system. This results in

$$<\Delta E_{si}(\underline{r}, t) \cdot \Delta \underline{E}_{si}^{*}(\underline{r}, t+\tau)> = \frac{\omega_o^4 \mu_o^2 z^4}{\pi^2 (\eta^2-1)^2 \rho_o^8} |F(\varphi_i)|^2 \int_{-h}^{o} dz_1 \int_{-h}^{o} dz_2 \, \gamma(z_1) \, \gamma^*(z_2)$$

$$e^{j2k_1 \sqrt{\eta^2 - 1} \, (z_1-z_2) + \frac{2\alpha(z_1+z_2)}{\sqrt{1-\eta^{-2}}}} \left[ \int_{\Delta S_i} d^2\bar{\rho} \int_{\Delta S_i} d^2\hat{\rho} \, C\left(|\hat{\rho}|, \, z_1, \, z_2, \, \tau\right) \right.$$

$$\left. e^{j2k_1 \underline{\rho}_{oi} \cdot \hat{\underline{\rho}}} \right] \tag{122}$$

where $\hat{\underline{\rho}} = \underline{\rho}_1 - \underline{\rho}_2$, $\bar{\underline{\rho}} = \frac{1}{2}(\underline{\rho}_1 + \underline{\rho}_2)$ and $\Delta S_i = \rho_o d \Delta \varphi_i$. In the transition from eq. (120) to (122) it has been assumed that the linear dimensions of $\Delta S_i$ (i.e., d, the range cell and $\rho_o \Delta \varphi_i$ are large compared to the transverse correlation length. It has been further assumed that the process $\epsilon(\underline{r}, t)$ is statistically homogeneous and isotropic in the transverse direction. The integration over $d^2\bar{\rho}$ is evaluated trivially resulting in $\Delta S_i$, while integration $d^2\hat{\rho}$ (for large $\Delta S_i$) is recognized as the Fourier transform of C with respect to $\hat{\rho}$ (i.e. the transverse spectral density function) to be denoted by

$$\hat{\Phi}(\underline{\kappa}, \, z_1, \, z_2, \tau) = \int C(\hat{\underline{\rho}}, \, z_1 \, z_2, \tau) \, e^{+j\underline{\kappa} \cdot \hat{\underline{\rho}}} d^2\hat{\rho} \tag{123}$$

Consequently, eq. (122) reduces to

$$<\underline{E}_{si}(\underline{r}, t) \cdot \Delta\underline{E}_{si}^{*}(\underline{r}, t+\tau)> = \frac{\omega_o^4 \mu_o^2 d z^4}{\pi^2 (\eta^2 - 1)^2 \rho_o^7} |F(\varphi_i)|^2 \Delta\varphi_i$$

$$\int_{-h}^{o} dz_1 \int_{-h}^{o} dz_2 \, \gamma(z_1) \, \gamma^*(z_2) \, \hat{\Phi}(2k_1, \, z_1, \, z_2, \tau)$$

$$e^{j2k_1 \sqrt{\eta^2 - 1} \, (z_1 - z_2) + \frac{2\alpha(z_1+z_2)}{\sqrt{1-\eta^{-2}}}} \tag{124}$$

42

Owing to the presumed transverse isotropy $\hat{\Phi}$ becomes an exclusive function of $\varkappa = |\underline{\varkappa}|$, and as is clear from eq. (122) it is the value of $\hat{\Phi}$ at $\varkappa = |2k_1 \underline{\rho}_{oi}| = 2k_1$, which is of interest.

The mean received power $(<P_r>)$ can now be calculated. From eq. (105) and the presumption of a matched antenna one has,

$$\langle P_r^{(i)} \rangle = \frac{\lambda^2}{4\pi} \left[ g(\varphi_i, \theta) \right]_{\theta \approx o} <S_i> = \frac{1}{2} \sqrt{\frac{\epsilon_o}{\mu_o}} \frac{\lambda^2}{4\pi} \left[ g(\varphi_i, \theta) \right]_{\theta \approx o} < |\Delta \underline{E}_{si}|^2 > \quad (125)$$

where $<S_i>$ denotes the mean Poynting vector at the receiving antenna; integration over the pattern yields

$$<P_r> = \frac{1}{2} \sqrt{\frac{\epsilon_o}{\mu_o}} \frac{\lambda^2}{4\pi} \frac{\omega_o^4 \mu_o^2 \, d \, z^4}{\pi^2 (\eta^2 - 1)^2 \rho_o^7} \left( \frac{1}{2\pi} \sqrt{\frac{\mu_o}{\epsilon_o}} P_t \right) \left[ \int_{-\pi}^{\pi} g^2(\varphi, \theta = o) \, d\varphi \right]$$

$$\int_{-h}^{o} dz_1 \int_{-h}^{o} dz_2 \, \gamma(z_1) \, \gamma^*(z_2) \, \hat{\Phi}(2k_1, z_1, z_2, \tau = o) \, e^{j2k_1 \sqrt{\eta^2 - 1} \, (z_1 - z_2) + \frac{2\alpha(z_1 + z_2)}{\sqrt{1 - \eta^{-2}}}} =$$

$$\frac{P_t \, dz^4 \left[ \int_{-\pi}^{+\pi} d\varphi \, g^2(\varphi) \right]}{\epsilon_o^2 \lambda^2 (\eta^2 - 1)^2 \rho_o^7} \int_{-h}^{o} dz_1 \int_{-h}^{o} dz_2 \, \gamma(z_1) \, \gamma^*(z_2) \, \hat{\Phi}(2k_1, z_1, z_2, \tau = o)$$

$$e^{j2k_1 \sqrt{\eta^2 - 1} \, (z_1 - z_2 + \frac{2\alpha(z_1 + z_2)}{\sqrt{1 - \eta^{-2}}}} \qquad (126)$$

Equation (126) may be further simplified if one is willing to except the assumptions that the medium is statistically homogeneous in z (i.e., $\hat{\Phi} = \hat{\Phi}(2k_1, z_1 - z_2, \tau)$), that the corresponding correlation length is small compared to the forest's effective height (h) and that ground effects are negligible. Arguments analogous to these used for the transverse domain lead to:

$$<P_r> \approx P_t \frac{dhz^4 \left[ \int_{-\pi}^{\pi} d\varphi \, g^2(\varphi) \right]}{\epsilon_o^2 \lambda^2 (\eta^2 - 1) \, \rho_o^7} \quad \frac{\sinh \frac{2\alpha h}{\sqrt{1-\eta^2}}}{\frac{2\alpha h}{\sqrt{1-\eta^{-2}}}} \quad e^{\frac{-2\alpha h}{\sqrt{1-\eta^{-2}}}} \quad \hat{\Phi}(2k_1, 2k_1 \sqrt{\eta^2 - 1}, \tau = 0)$$

$$(127)$$

where,

$$\hat{\Phi}(2k_1, 2k_1\sqrt{\eta^2-1}, \tau = 0) \approx \int_{-\infty}^{+\infty} dz \; e^{j2k_1\sqrt{\eta^2-1}\,\hat{z}} \; \hat{\hat{\Phi}}(2k_1, \hat{z}, \tau = 0), \quad \hat{z} = z_1 - z_2$$

It should be pointed out that the assumptions allowing the transition from eq. (126) to eq. (127) may be seriously challenged. However, the ensuing simplifications are substantial indeed.

Equation (127) indicates that the mean received power decreases as the seventh power of the range. Experimental verification of this dependence is demonstrated in Fig. 9 which is a plot of received clutter power as a function of range at UHF for a uniform pine forest.

The scattered field given in eq. (117) or (118) constitutes (via the central limit theorem) a normal process provided that $V_s$ (or $\Delta V_i$), the scattering volume, is dimensionally large in comparison with the correlation distance characterizing $\epsilon(\underline{r}, t)$. It can be shown (see Appendix) that the processes $\underline{E}_1 = R_e(\Delta\underline{E}_{si})$ and $\underline{E}_2 = Im(\Delta\underline{E}_{si})$ are normally distributed with equal variance (to be denoted by $\sigma_E^2$) and are uncorrelated. From which it follows that the field's amplitude $(A_i)$ and phase are describable by Rayleigh and uniform distributions, respectively. Consequently (see Appendix),

$$Var\,[A_i^2] \equiv <[A_i^2 - <A_i^2>]^2> = <A_i^2>^2$$
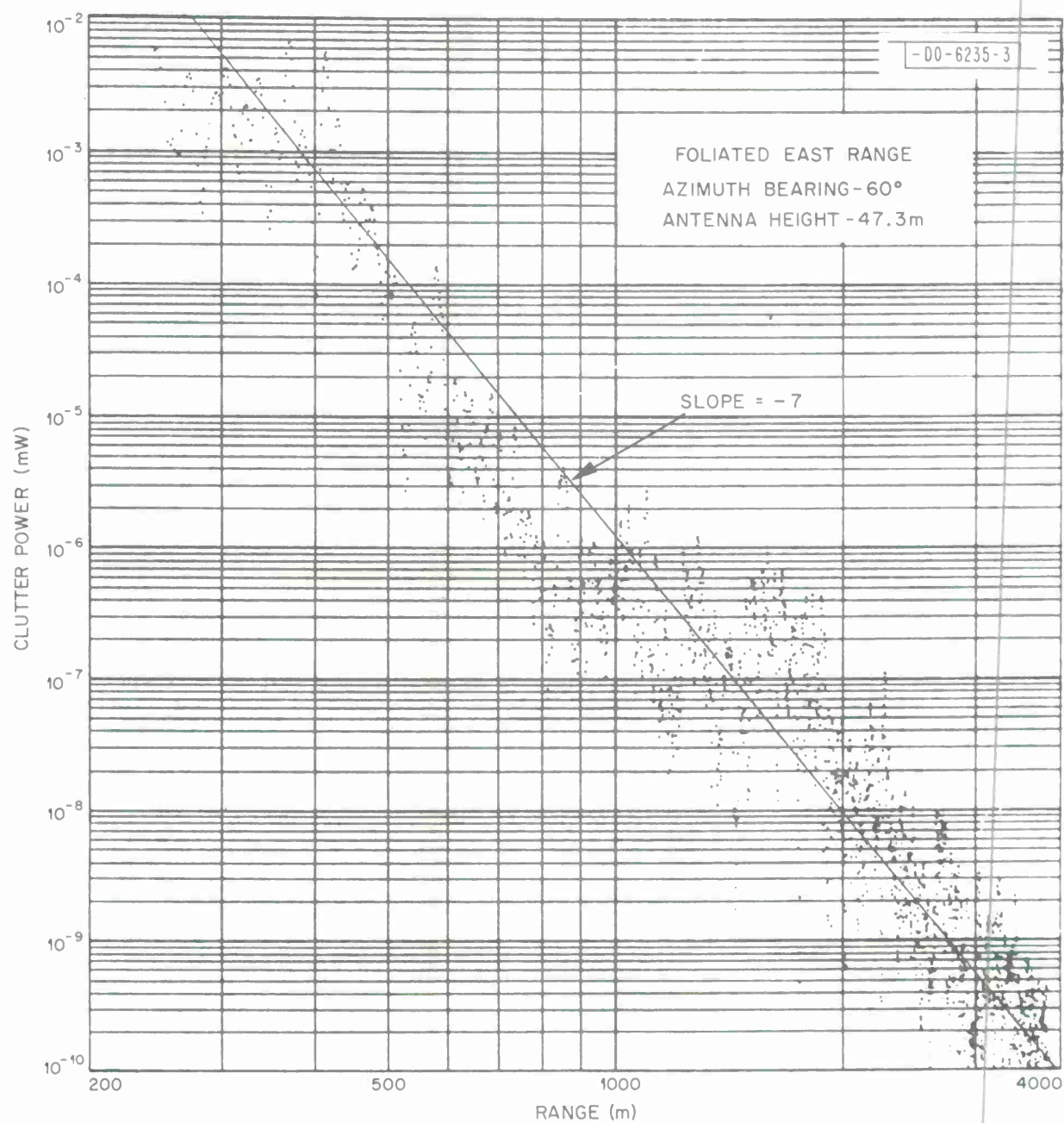
or

$$Var\,[P_r] \equiv <[P_r - <P_r>]^2> = <P_r>^2$$

44

Fig. 9.   Clutter power vs range.

where $<P_r>$, the mean power, is given in equations (126) or (127).

All information concerning the field's temporal correlation or its spectrum is contained in the normalized function.

$$C_E(\tau) = M \int_{-h}^{o} dz_1 \int_{-h}^{o} dz_2 \; \gamma(z_1) \; \gamma^*(z_2) \hat{\Phi} \; (2k_1, z_1, z_2, \tau)$$

$$e^{j2k_1 \sqrt{1-\eta^2}} (z_1 - z_2) + \frac{2\alpha}{\sqrt{1-\eta^{-2}}} (z_1 + z_2) \tag{128}$$

where M is a normalization constant, conveniently selected in accord with the condition $C_E(o) = 1$.

## E.   THE CLUTTER SPECTRUM

This section is reserved to a further investigation of $C_E(\tau)$ as given by eq. (128) and the associated spectral density under various circumstances to be specified below.

The temporal fluctuations associated with the random process $\epsilon(\underline{r}, t)$ can be thought of as caused by the motion of distributed scatterers characterized by a random velocity field $\underline{V}(\underline{r}, t)$.  Thus, assuming a conservative ensemble of scatterers (that is, assume that no scattering centers disappear from the collection) one concludes that the relationship

$$\epsilon(\underline{r}, t+\tau) = \epsilon(\underline{r} - \int_{t}^{t+\tau} \underline{V}(\underline{r}, s) \; ds, t) \tag{129}$$

is satisfied.  It is further assumed that the processes $\epsilon(\underline{r})$ and $\underline{V}(\underline{r}, t)$ are statistically independent.  This assumption is not totally baseless since the fluctuations of $\epsilon$ are primarily a consequence of the spatial distribution of the vegetation (and therefore virtually independent of wind conditions) while the

46

nature of $\underline{V}$ depends greatly upon prevailing winds. As a result the averaging over the processes $\epsilon$ and $\underline{V}$ can be carried sequentially. One has,

$$C(\underline{R}, \ \underline{r}, \ \tau) = \ < \epsilon(\underline{r}, t) \ \ \epsilon(\underline{r}+\underline{R}, t+\tau)> =$$

$$<< \epsilon(\underline{r}, t) \ \ \epsilon(\underline{r}+\underline{R} - \int_{t}^{t+\tau} \underline{V}(\underline{r}+\underline{R}, \ s) \ ds, t) >_{\epsilon} > \ \underline{V} =$$

$$< C_{\epsilon}(\underline{R} - \int_{t}^{t+\tau} \underline{V}(\underline{r}+\underline{R}, \ s) \ ds) > \ \underline{V} \tag{130}$$

where the process $\epsilon$ was presumed statistically homogeneous and stationary. Let $\Phi_{\epsilon}$ denote the (spatial) spectral density corresponding to $C_{\epsilon}$. It follows from eq. (130) that

$$C(\underline{R}, \underline{r}, \tau) = \frac{1}{(2\pi)^3} \int d^3\kappa \, \Phi_{\epsilon}(\underline{\kappa}) \ e^{-j\underline{\kappa} \cdot \ \underline{R}} \ < e^{+j\kappa \int_{0}^{\tau} ds \ V_{\kappa}(\underline{r}+\underline{R}, s)} > \ \underline{V} \tag{131}$$

where $V_{\kappa}$ denotes the velocity component along $\underline{\kappa}$ and the integration range $t \leq s \leq t+\tau$ was shifted to $o \leq s \leq \tau$ in view of the presumed statistical stationarity of the process $\underline{V}(\underline{r}, t)$. If the process $\underline{V}$ is also transversely homogeneous, the term $< >_{\underline{V}}$ in eq. (131) becomes independent of the transversely homogeneous the ordinates (but is generally a function of the vertical coordinate). Separating the transverse integration from the longitudinal eq. (131) may be written in the form:

$$C(\underline{R}, \underline{r}, \tau) = \frac{1}{(2\pi)^2} \int d^2\kappa_t \ e^{-j\underline{\kappa}_t \cdot \ \widehat{\underline{\rho}}} \left[ \frac{1}{2\pi} \int_{-\infty}^{+\infty} d\kappa_z \ e^{-j\kappa_z \widehat{z}} \, \Phi_{\epsilon}(\underline{\kappa}_t, \underline{\kappa}_z) \right.$$

$$\left. < e^{j\kappa \int_{0}^{\tau} ds \ V_{\kappa}(\underline{r}+\underline{R}, \ s)} > \ V \right] \tag{132}$$

47

Using the notation of eq. (123),

$$C(\underline{R}, \underline{r}, \tau) = C(\hat{\underline{\rho}}, z_1, z_2, \tau) = \frac{1}{(2\pi)^2} \int\limits_{-\infty}^{+\infty} d^2\varkappa_t \ e^{-j\underline{\varkappa}_t \cdot \hat{\underline{\rho}}} \ \hat{\Phi}(\underline{\varkappa}_t, z_1, z_2, \tau) \quad (133)$$

hence, (the bracketed term in eq. (132) is presumed to be independent of $\hat{\underline{\rho}}$)

$$\hat{\Phi}(\underline{\varkappa}_t, z_1, z_2, \tau) = \frac{1}{2\pi} \int\limits_{-\infty}^{+\infty} d\varkappa_z \ e^{-j\varkappa_z \hat{z}} \ \Phi_\epsilon(\underline{\varkappa}_t, \varkappa_z) <e^{j\varkappa \int\limits_0^\tau ds \ V_\varkappa(\underline{r}+\underline{R}, s)}>_V \quad (134)$$

Owing to the near grazing incidence of the wave we know that the major contributions will come from ranges in which $\varkappa_z << |\underline{\varkappa}_t|$ (see for example eq. (127) in which $k_z / |\underline{k}_t| \approx \sqrt{1-\eta^2}$. Hence, $\varkappa$ in the exponent of eq. (134) can be replaced by $\varkappa_t$ and as a result one has,

$$\hat{\Phi}(\underline{\varkappa}_t, z_1, z_2, \tau) \approx \Phi_\epsilon(\underline{\varkappa}_t, \hat{z}) \ < e^{j\varkappa_t \int\limits_0^\tau ds \ V_\varkappa(\underline{r}+\underline{R}, s)}>_{\underline{V}} \quad (135)$$

where

$$\Phi_\epsilon(\underline{\varkappa}_t, \hat{z}) = \frac{1}{2\pi} \int\limits_{-\infty}^{+\infty} d\varkappa_z \ e^{-j\varkappa_z \hat{z}} \ \Phi_\epsilon(\underline{\varkappa}_t, \varkappa_z) = \int d^2\hat{\rho} \ C_\epsilon(\hat{\underline{\rho}}, \hat{z}) \ e^{+j\underline{\varkappa}_t \cdot \hat{\underline{\rho}}} \quad (136)$$

The substitution of eq. (135) into eq. (128) (with $\varkappa_t = 2k_1$) yields

$$C_E(\tau) = M \int\limits_{-h}^0 dz_1 \int\limits_{-h}^0 dz_2 \ \gamma(z_1) \ \gamma^*(z_2) \ \Phi_\epsilon(2k_1, \hat{z}) \ e^{j2k_1 \sqrt{1-\eta^2} \hat{z} + \frac{2\alpha}{\sqrt{1-\eta^{-2}}} (z_1+z_2)}$$

$$<e^{j2k_1 \int\limits_0^\tau ds \ V_\varkappa(\underline{r}+\underline{R}, s)}>_V \quad (137)$$

or upon transforming with respect to $\tau$:

48

$$\Phi_E(\omega) = \int_{-\infty}^{+\infty} d\tau \ e^{-j\omega\tau} \ C_E(\tau) =$$

$$M \int_{-h}^{0} dz_1 \int_{-h}^{0} dz_2 \ \gamma(z_1) \gamma^*(z_2) \ \Phi_\epsilon(2k_1, \hat{z}) \ e^{j2k_1 \sqrt{1-\eta^2} \ \hat{z} + \frac{2\alpha}{\sqrt{1-\eta^{-2}}} \ (z_1+z_2)}$$

$$< \int_{-\infty}^{+\infty} d\tau \ e^{-j\omega\tau + j2k_1 \int_{0}^{\tau} ds \ V_\varkappa(\underline{r}+\underline{R}, s)} >_V \tag{138}$$

Eqs. (137) and (138) still constitute rather complicated forms. Several options are open for their further reduction of which two are discussed below.

1. First Option

The averaging process over $\underline{V}$ can be carried out explicitly under the assumption that

$$\rho_\varkappa(\underline{r}, \tau) = \int_{0}^{\tau} ds \ V_\varkappa(\underline{r}, s) \tag{139}$$

is a multivariate Gaussian process. The Gaussian character of $\rho_\varkappa$ cannot be generally justified unless $\tau$ is large compared to the correlation time $(\tau_c)$ of $V_\varkappa$. For $\tau \gg \tau_c$ $\rho_\varkappa$ is Gaussian, owing to the central limit theorem, regardless of the precise characterization of $V_\varkappa$. In the range $\tau \leq \tau_c$, $\rho_\varkappa$ is Gaussian only if $V_\varkappa$ is. We have

$$<e^{j2k_1 \ \rho_\varkappa(\underline{r}, \tau)}>_V = e^{-2k_1^2 <\rho_\varkappa^2>_V} = e^{-2k_1^2 \int_{0}^{\tau} ds_1 \int_{0}^{\tau} ds_2 \ <V_\varkappa(\underline{r}, s_1) V_\varkappa(\underline{r}, s_2)>_{\underline{V}}} =$$

$$e^{-4k_1^2 \int_{0}^{\tau} d\hat{s} \ (\tau-\hat{s}) \ C_V(\underline{r}, \hat{s})} \tag{140}$$

where, $\hat{s} = s_1 - s_2$ and $C_V(\underline{r}, \hat{s}) = <V_\varkappa(\underline{r}, s_1) V_\varkappa(\underline{r}, s_2)>$. The process $\underline{V}$ has been

49

presumed to be transversely homogeneous. Consequently, $C_V$ is a function of z only. If we also assume that the vertical inhomogeneity affects primarily the variance of the $\underline{V}$ fluctuations but not other correlation features such as $\tau_c$, it follows that

$$C_V(\underline{r}, \hat{s}) = <V_\varkappa^2(z)> \, f_V(\hat{s}) \tag{141}$$

where $f_V(s)$ denotes the correlation coefficient of the velocity field. The substitution of eqs. (140) and (141) into (138) yields,

$$\Phi_E(\omega) = M \int_{-h}^{0} dz_1 \int_{-h}^{0} dz_2 \, \gamma(z_1) \, \gamma^*(z_2) \, \Phi_\epsilon(2k_1, \hat{z}) \, e^{j2k_1 \sqrt{1-\eta^2}\,\hat{z} + \frac{2\alpha}{\sqrt{1-\eta^{-2}}}(z_1+z_2)}$$

$$\left[ \int_{-\infty}^{+\infty} d\tau e^{-j\omega\tau} - 4k_1^2 <V_\varkappa^2(z_2)> \int_{0}^{\tau} d\hat{s} \, (\tau-\hat{s}) \, f_V(\hat{s}) \right] \tag{142}$$

or alternatively,

$$\Phi_E(\omega) = M \int_{-h}^{0} dz_1 \int_{-h}^{0} dz_2 \, \gamma(z_1) \, \gamma^*(z_2) \, \Phi_\epsilon(2k_1, \hat{z}) \, e^{j2k_1 \sqrt{1-\eta^2}\,\hat{z} + \frac{2\alpha}{\sqrt{1-\eta^{-2}}}(z_1+z_2)}$$

$$\left[ \int_{-\infty}^{+\infty} d\tau \, e^{-j\omega\tau} - 4k_1^2 <V_\varkappa^2(z_2)> \tau^2 \int_{0}^{\infty} d\xi \, \Phi_V(\xi) \left[ \frac{\sin\frac{\xi\tau}{2}}{\frac{\xi\tau}{2}} \right]^2 \right] \tag{143}$$

where

$$\Phi_V(\xi) = \frac{1}{2\pi} \int_{-\infty}^{+\infty} d\hat{s} \, f_V(\hat{s}) \, e^{-j\xi\hat{s}} \tag{144}$$

represents the spectral-density of the velocity field. If we further assume that $<V_\varkappa^2>$ does not vary (or varies slowly) over the contributing range of z,

one observes that the bracketed terms in eqs. (142) or (143) are independent of $z_1$ and $z_2$. These terms, which may be taken out of the respective integrals, completely determine the normalized field's spectrum:

$$\hat{\Phi}_E(\omega) = \hat{M} \int_{-\infty}^{+\infty} d\tau \ e^{-j\omega\tau} \ e^{-4k_1^2 <V_{\varkappa}^2>} \int_0^{\tau} d\hat{s} \ (\tau - \hat{s}) \ f_V(\hat{s}) =$$

$$\hat{M} \int_{-\infty}^{+\infty} d\tau \ e^{-j\omega\tau} \ e^{-4k_1^2 <V_{\varkappa}^2>} \ \tau^2 \int_0^{\infty} d\xi \ \Phi_V(\xi) \left( \frac{\sin \frac{\xi\tau}{2}}{\frac{\xi\tau}{2}} \right)^2 \qquad (145)$$

with $\hat{M}$ selected so that $\quad \dfrac{1}{2\pi} \displaystyle\int_{-\infty}^{+\infty} d\omega \ \hat{\Phi}_E(\omega) = 1.$

The asymptotic behavior of $\hat{\Phi}_E(\omega)$ for large and small $\omega$ (small and large $\tau$, respectively) can be readily determined. These asymptotic observations are of special significance since they are independent of the detailed form of $f_V(\hat{s})$.

(a) The limit $\omega \to 0 \ (\tau >> \tau_c)$.

The major contributions to the $d\hat{s}$ integral in the exponential of eq. (145) comes from the range $\hat{s} \le \tau_c$. hence

$$\int_0^{\tau} d\hat{s} \ (\tau - \hat{s}) \ f_V(\hat{s}) \approx |\tau| \int_0^{\infty} d\hat{s} \ f_V(\hat{s}) = |\tau| \ \tau_c \qquad (146)$$

$$\lim_{\omega \to 0} \hat{\Phi}_E(\omega) = \hat{M} \int_{-\infty}^{+\infty} d\tau \ e^{-j\omega\tau} \ e^{-4k_1^2 <\bar{V}_{\varkappa}^2> \tau_c |\tau|} = \frac{\hat{\Phi}_E(0)}{1 + (\frac{\omega}{\omega_1})^2} \qquad (147)$$

it follows that

$$\hat{M} = 2k_1^2 <\bar{V}_{\varkappa}^2> \tau_c \ \hat{\Phi}_E(0) = 1, \ \hat{\Phi}_E(0) = 2/\omega_1 \qquad (148)$$

51

and the defining identities

$$\tau_c \equiv \int_0^\infty d\hat{s}\, f_V(\hat{s}) = \pi\, \hat{\Phi}_V(0) \tag{149}$$

$$\omega_1 = 4k_1^2 < V_{\varkappa}^2 > \tau_c \tag{150}$$

have been introduced.

Comment: The bound character of the vegetation's scattering centers (i.e., the finite variance of their displacement in the limit $\tau \rightarrow \infty$) implies a DC return which is totally ignored in the above sequence.

(b) The limit $\omega \rightarrow \infty$ ($\tau \ll \tau_c$).

In the range $0 \le s << \tau_c$ the correlation function $f_V(s)$ stays virtually constant:

$$f_V(\hat{s}) \approx f_V(0) = 1 \tag{151}$$

hence,

$$\lim_{\omega \rightarrow \infty} \hat{\Phi}_E(\omega) = \hat{M} \int_{-\infty}^{+\infty} d\tau\, e^{-j\omega\tau}\, e^{-2k_1^2 < V_{\varkappa}^2 > \tau^2} = \hat{\Phi}_E(0)\, \frac{\sqrt{\pi\omega_1\tau_c}}{2}\, e^{-\frac{\omega_1\tau_c}{2}(\frac{\omega}{\omega_1})^2} \tag{152}$$

The transition curve connecting the asymptotic segments described by eqs. (147) and (152) is complicated by its dependence on the detailed form of $f_V(\tau)$. $f_V(\tau)$, while a relatively simple characterization of the coupling between the mechanical motion of the forest scatterers and the turbulent wind is an unknown. Little reliable data exists which may allow its determination. It must be either assumed or derived on the basis of some simple (and probably over simplified) models. For example, one may regard the wind-forest interaction as that between a harmonic oscillator and an isotropic and homogeneous turbulent wind (M. Labitt and R. Yates, private communication).

52

Alternatively, one can assume that regardless of the driving (wind) forces the resulting motion can be approximately viewed as locally harmonic over the relevant time interval. This option is discussed in the second part of this section. The form

$$f_v(\tau) = f_d(\tau) \, f_o(\tau) \tag{153}$$

where $f_d(\tau)$ and $f_o(\tau)$ denote decaying and periodic functions respectively, is suggestive (although not rigorously defensible). As an example, selected for its relative simplicity, one can take the form

$$f_V(\tau) = e^{-\frac{|\tau|}{\tau_o}} \cos \bar{\Omega} \tau \tag{154}$$

which permits the explicit evaluation of the integral:

$$\int_o^\tau (\tau - \hat{s}) \, f_V(\hat{s}) \, d\hat{s} = \frac{\tau_o^2}{1+\bar{\Omega}^2 \tau_o^2} \left[ \frac{|\tau|}{\tau_o} - \cos \beta + e^{-|\tau|/\tau_o} \cos(\beta + \bar{\Omega} |\tau|) \right] \tag{155}$$

where

$$\cos \beta = \frac{1-\bar{\Omega}^2 \tau_o^2}{1+\bar{\Omega}^2 \tau_o^2} , \quad o < \beta = \cos^{-1} \frac{1-\bar{\Omega}^2 \tau_o^2}{1+\bar{\Omega}^2 \tau_o^2} < \pi \tag{156}$$

$$\sin \beta = \frac{2\bar{\Omega} \tau_o}{1+\bar{\Omega}^2 \tau_o^2} \tag{157}$$

$\tau_c$ is defined in eq. (149) and is related to $\bar{\Omega}$ and to $\tau_o$ via[*]

$$\tau_c = \frac{\tau_o}{1+\bar{\Omega}^2 \tau_o^2} \tag{158}$$

The substitution of eq. (155) into eq. (145) with $\hat{M}$ given by eq. (148) results in:

[*]Although $\tau_c$ as given by eq. (158) should not be strictly interpreted as a measure of the correlation time of the velocity field of eq. (154), it is convenient to preserve the definition given by eq. (149).

53

$$\hat{\Phi}_E(\omega) = 2k_1^2 \ \hat{\Phi}_E(0) < \bar{V}_\varkappa^2 > \tau_c \int_{-\infty}^{+\infty} d\tau \ e^{-j\omega\tau}$$

$$e^{-4k_1^2 < \bar{V}_\varkappa^2 > \tau_o \tau_c} \left[ \frac{|\tau|}{\tau_o} - \cos \beta + e^{-|\tau|/\tau_o} \cos (\beta + \bar{\Omega} |\tau|) \right]^* \tag{159}$$

One immediate conclusion stemming from eq. (159) is that even for the simple choice (154) no closed form expression for $\hat{\Phi}_E(\omega)$ is available. The Fourier transform (159) was evaluated on a computer and examples of these results are shown in Fig. 10. The theoretical result given by the solid curve ($\bar{\Omega}\tau_o = 5$, $\omega_1\tau_o = 0.5$) is very similar to measured UHF clutter spectra with moderate winds.

2. An Alternative Option

The forthcoming analysis starts once again with eq. (138). However, instead of presuming the process $V_\varkappa(\underline{r}, t)$ to be normal we now postulate a locally harmonic temporal dependence:

$$V_\varkappa(\underline{r}, t) = V_m(\underline{r}) \cos [\Omega (\underline{r})t + \varphi (\underline{r})] \tag{160}$$

where $V_m(\underline{r})$, $\Omega(\underline{r})$ and $\varphi(\underline{r})$ are random functions of $\underline{r}$ but are time independent. The relation (160) is not expected to constitute a valid description over prolonged periods. The resulting spectral predictions, therefore, are expected to be inaccurate near DC. In this respect, the model to be pursued in this section can be regarded as complementary to that leading to eq. (147). It follows trivially that,

$$\int_o^\tau V_\varkappa (\underline{r}, \hat{s}) \ d\hat{s} = \rho_m(\underline{r}) [\sin \Omega \tau + \varphi) - \sin\varphi] \tag{161}$$

where $V_m$ and $\rho_m = V_m/\Omega$ represent local maxima of $V_\varkappa$ and the displacement,

---

*Vanishing of the field as $\tau \to \infty$ implies unbound scatterers. We are aware that the scatterers are indeed bounded but here have chosen to disregard this feature since the loss of a measure of the stationary backscatter (impulse at $\omega = o$) is not a major penalty.
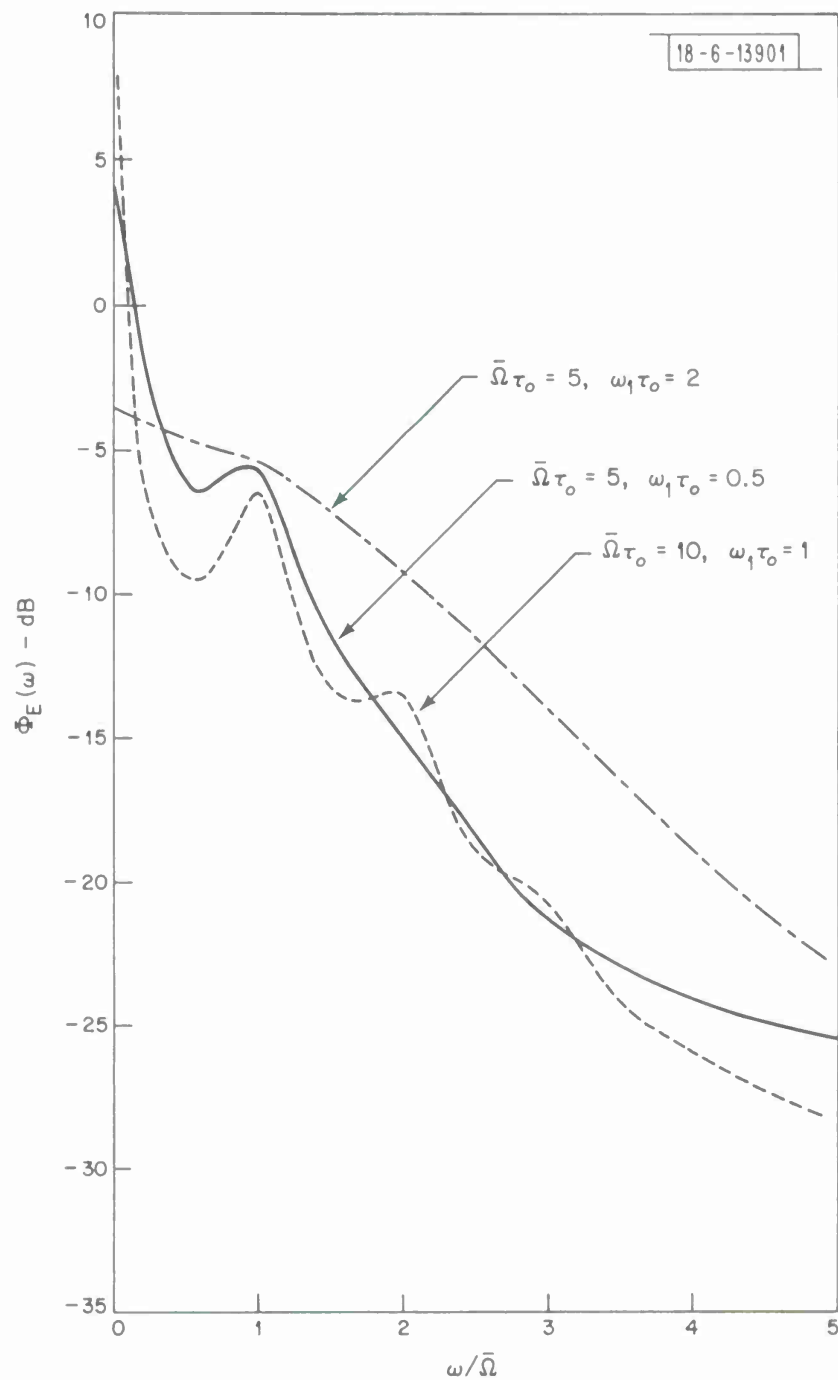
Fig. 10.   Clutter spectral density.

respectively, If we assume $\rho_m$, $\Omega$ and $\varphi$ to be statistically independent (not entirely unreasonable since $\Omega$ and $\varphi$ are expected to be essentially independent of wind conditions, while a strong wind dependence is anticipated for $\rho_m$), one obtains

$$I_E(\omega) \equiv \left\langle \int_{-\infty}^{+\infty} d\tau \; e^{-j\omega\tau \,+\, j2k_1 \int_0^\tau ds \, V_\varkappa(\underline{r}, s)} \right\rangle_V =$$

$$\left\langle e^{-j2k_1 \, \rho_m(\underline{r}) \, \sin \varphi} \int_{-\infty}^{+\infty} d\tau \; e^{-j\omega\tau \,+\, j2k_1 \, \rho_m(\underline{r}) \, \sin(\Omega\tau + \varphi)} \right\rangle_{\substack{\rho_m \\ \varphi \\ \Omega}} \qquad (162)$$

where $I_E(\omega)$ is defined by the expression to its right, and $\langle \; \rangle_{\substack{\rho_m \\ \varphi \\ \Omega}}$

indicates sequential averaging over the distributions of $\rho_m$, $\varphi$, and $\Omega$ (the actual averaging sequence is arbitrary). The substitution of the expansion

$$e^{j2k_1 \, \rho_m \, \sin(\Omega\tau + \varphi)} = \sum_{n=-\infty}^{+\infty} J_n(2k_1 \, \rho_m) \; e^{jn(\Omega\tau + \varphi)} \qquad (163)$$

into eq. (162) and carrying out the $\tau$ - integration results in

$$I_E(\omega) = 2\pi \left\langle e^{-j2k_1 \, \rho_m \, \sin \varphi} \sum_{n=-\infty}^{\infty} J_n(2k_1 \, \rho_m) \; e^{jn\varphi} \, \delta(\omega - n\Omega) \right\rangle_{\substack{\rho_m \\ \varphi \\ \Omega}} \qquad (164)$$

The averaging over $\varphi$ is readily performed if we presume a uniform distribution within the interval $-\pi < \varphi < \pi$:

$$\left\langle e^{-j2k_1 \, \rho_m \, \sin \varphi \,+\, jn\varphi} \right\rangle_\varphi = \frac{1}{2\pi} \int_{-\pi}^{\pi} d\varphi \; e^{-j2k_1 \, \rho_m \, \sin \varphi \,+\, jn\varphi} \equiv J_n(2k_1 \, \rho_m) \qquad (165)$$

56

Eq. (164) is reduced to

$$I_E(\omega) = 2\pi \sum_{n=-\infty}^{\infty} \langle J_n^2 (2k_1 \, \rho_m) \rangle_{\rho_m} \langle \delta(\omega - n\Omega) \rangle_\Omega =$$

$$2\pi \langle J_o^2 (2k_1 \, \rho_m) \rangle_{\rho_m} \delta(\omega) + 2\pi \sum_{n=1}^{\infty} \langle J_n^2 (2k_1 \rho_m) \rangle_{\rho_m} \langle \delta(\omega - n\Omega) + \delta(\omega + n\Omega) \rangle_\Omega \quad (166)$$

Let $P(\Omega)$ denote the density function specifying the $\Omega$ distribution (its general properties are discussed below). The $\Omega$ averaging leads to

$$I_E(\omega) = 2\pi \langle J_o^2 (2k_1 \rho_m) \rangle_{\rho_m} \delta(\omega) +$$

$$2\pi \sum_{n=1}^{\infty} \frac{1}{n} \langle J_n^2 (2k_1 \, \rho_m) \rangle_{\rho_m} [P(\frac{\omega}{n}) + P(-\frac{\omega}{n})] \quad (167)$$

It can be immediately observed that $I_E(\omega)$ is symmetric about $\omega = o$, regardless of the precise nature of $P(\Omega)$.

The task of averaging over $\rho_m$ is more difficult. However, before turning to it we discuss some of the properties of eq. (167) which are relatively insensitive to the term $< J_n^2 (2k_1 \, \rho_m) > _{\rho_m}$.

$P(\Omega)$ is not known. However, since it essentially describes the distribution of resonance frequencies (positive by definition) of the ensemble of forest constituents it must vanish in the limits $\Omega \to \infty$ and $\Omega \le o$. It must contain at least one maximal value; for simplicity let us assume that $P(\Omega)$ possesses a single maximum (say at $\Omega = \Omega_o$).

The physical interpretation of eq. (167) is straightforward. It contains two distinct parts. The first (in our case proportional to $\delta(\omega)$) represents

that part of the received power which did not undergo spectral modifications. Its spectral content is identical to that of the transmitted signal, although it experiences a power reduction (represented by the coefficient $<J_o^2(2k_1\rho_m)>$) as the power conversion process into other spectral constituents (represented by the second term in eq. (167)) becomes more efficient. The efficiency of this conversion process depends primarily on the (random) parameter $k_1\rho_m$. Under no wind conditions ($k_1\rho_m = 0$) all the power is contained in the first (DC) term. The second term vanishes. As $k_1\rho_m$ increases (with the rising magnitude of wind velocity), the DC term decreases in magnitude, the second term increases, consistently with the anticipated conservation of energy. The singular character, of the DC term, stems directly from the presumed monochromatic nature of the transmitted signal. Eq. (167) stays valid if the actual, distributed spectrum of the transmitted signal replaces the $\delta$-function, provided that it is sharply peaked (on the scale of $\Omega_o$).

The spectral-density $\Phi_E(\omega)$ can be obtained now by the substitution of eq. (167) into eq. (138). However, because of the complexity of the result we presently assume $\rho_m$ to be statistically homogeneous in all directions. Consequently, $I_E(\omega)$ is independent of $z_1$ and $z_2$ and represents by itself the desired spectral density.

We now turn to the estimate of the coefficients $<J_n^2(2k_1\rho_m)>_{\rho_m}$ in the limits of weak ($k_1\rho_m << 1$) and strong ($k_1\rho_m >> 1$) winds.

(a) The limiting case $k_1\rho_m << 1$.

The Bessel functions may be replaced by the term in the corresponding power series expansion:

58

$$\langle J_n^2 (2k_1 \rho_m) \rangle_{\rho_m} \approx \frac{\langle (k_1 \rho_m)^{2n} \rangle_{\rho_m}}{(n!)^2} \qquad (168)$$

The series is a rapidly convergent one and for

$$\langle (k_1 \rho_m)^2 \rangle_{\rho_m} >> \frac{1}{8} \langle (k_1 \rho_m)^4 \rangle_{\rho_m} \qquad (169)$$

it is properly represented by its first term:

$$I_E(\omega) \approx I_E^{(o)}(\omega) + 2\pi \langle (k_1 \rho_m)^2 \rangle_{\rho_m} [P\omega) + P(-\omega)] \qquad (170)$$

where $I_E^{(o)}$ represents $I_E(\omega)$ measured under no wind conditions ($\rho_m \equiv o$). In eq. (167), $I_E^{(o)}(\omega)$ is identified as $2\pi \delta(\omega)$.

The presumption of validity of the above model indicates the feasibility of the experimental determination of $P(\omega)$ from the measurement of $I_E(\omega)$ under weak wind conditions. From eq. (170) one has

$$P(\omega) \approx C [I_E(\omega) - I_E^{(o)}(\omega)] U(\omega) \qquad (171)$$

where C is selected consistently with the requirement: $C \int_0^\infty [I_E(\omega) - I_E^{(o)}(\omega)] d\omega = 1$.
The experimental determination of $P(\omega)$ via eq. (171) is significant owing to the anticipated insensitivity of $P(\omega)$ to varying wind conditions. The determined $P(\omega)$ may be utilized in eq. (167) for relatively arbitrary winds.

(b) The limiting case $k_1 \rho_m >> 1$. An exact evaluation of $\langle J_n^2 (2k_1 \rho_m) \rangle_{\rho_m}$.

It will be found advantageous to represent the Bessel functions in eq. (167) by their integral representation. We have,

$$< J_n^2 \, (2k_1 \, \rho_m) >_{\rho_m} \; \equiv \; \frac{1}{4} \, < \, [(H_n^{(1)} \, (2k_1 \rho_m) + H_n^{(2)} \, (2k_1 \, \rho_m)\,]^2 >_{\rho_m} \; =$$

$$\frac{1}{4} \, <H_n^{(1)^2} \, (2k_1 \, \rho_m) + H_n^{(2)^2} \, (2k_1 \, \rho_m) + 2 \, H_n^{(1)} (2k_1 \, \rho_m) \, H_n^{(2)} \, (2k_1 \, \rho_m)>_{\rho_m} \qquad (172)$$

where the Hankel function is defined via

$$H_n^{\binom{1}{2}} \, (2k_1 \, \rho_m) = \frac{1}{\pi} \, \int\limits_{C_{\frac{1}{2}}} e^{-j2k_1 \, \rho_m \, \sin \varphi \, + \, jn\varphi} \; d\varphi \qquad (173)$$

and the paths $C_{\frac{1}{2}}$ are illustrated in Fig. 11. For simplicity we assume $\rho_m$ to be normally distributed with a mean $\bar{\rho}_m$ and a variance $\sigma_\rho = <(\rho_m - \bar{\rho}_m)^2 >^{1/2}$. If we further define the parameters:

$$L = [ \, (2k_1 \, \bar{\rho}_m)^2 + (2k_1^2 \, \sigma_\rho^2)^2\,]^{1/2} \, , \; \sin \alpha = \frac{2k_1 \, \bar{\rho}_m}{L} \, , \; o < \alpha < \frac{\pi}{2} \qquad (174)$$

we find,

$$<H_n^{\binom{1}{2}^2} \, (2k_1 \, \rho_m) >_{\rho_m} = \frac{1}{\pi^2} \, \int\limits_{C_{\frac{1}{2}}} d\varphi_1 \int d\varphi_2 \; e^{jn(\varphi_1 + \varphi_2)} \, e^{-LQ(\varphi_1, \; \varphi_2)} \qquad (175)$$

and

$$<H_n^{(1)} \, (2k_1 \rho_m) \, H_n^{(2)} \, (2k_1 \rho_m) >_{\rho_m} = \frac{1}{\pi^2} \, \int\limits_{C_1} d\varphi_1 \int\limits_{C_2} d\varphi_2 \; e^{jn(\varphi_1 + \varphi_2) \, - \, LQ(\varphi_1, \, \varphi_2)}$$

$$\qquad (176)$$

where

$$Q(\varphi_1, \varphi_2) = j \sin \alpha \, (\sin \varphi_1 + \sin \varphi_2) + \cos \alpha \, (\sin \varphi_1 + \sin \varphi_2)^2 \qquad (177)$$

Eqs. (175) and (176) are now evaluated asymptotically (with L taken to be
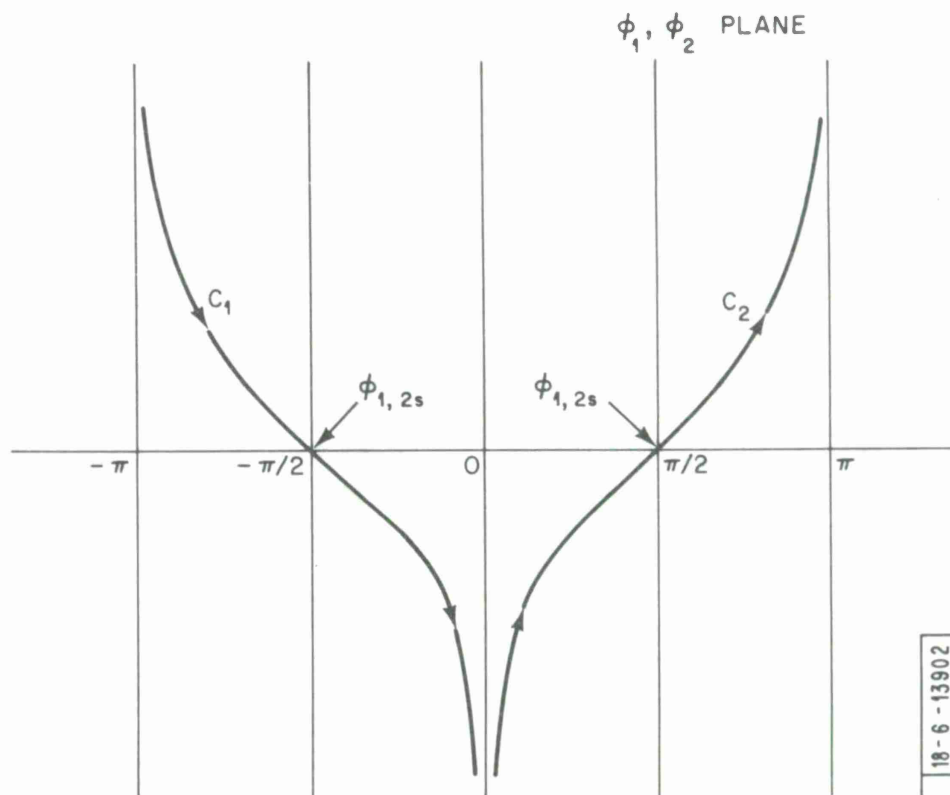
Fig. 11.   The path defining $H_n(\frac{1}{2})$.

the large parameter) via the method of steepest descent. The saddle points $\varphi_{1s}$ and $\varphi_{2s}$ defined by the equations

$$\frac{\partial Q\,(\varphi_{1s},\,\varphi_{2s})}{\partial \varphi_{1s}} \;=\; 0 \;=\; \frac{\partial Q\,(\varphi_{1s},\,\varphi_{2s})}{\partial \varphi_{2s}} \tag{178}$$

are readily found to be situated at either $+\frac{\pi}{2}$ ( on $C_2$ ) or at $-\frac{\pi}{2}$ (along $C_1$).
Eq. (175) yields the saddle-point contribution.

$$< H_n^{\binom{1}{2}^2} (2k_1 \rho_m) >_{\rho_m} \;\sim\; \frac{2\pi}{L} \; \frac{e^{jn(\varphi_{1s} + \varphi_{2s})}}{\left[ \dfrac{\partial^2 Q}{\partial \varphi_1^2} \; \dfrac{\partial^2 Q}{\partial \varphi_2^2} \right]^{1/2}} \; e^{-LQ(\varphi_{1s},\,\varphi_{2s})} + O\left(\frac{1}{L^3}\right)$$
$$\begin{matrix} \varphi_1 = \varphi_{1s} \\ \varphi_2 = \varphi_{2s} \end{matrix}$$

$$\approx \; \frac{2\pi}{L} \; \frac{e^{\mp jn\pi - L\,(4\cos\alpha \mp 2j\sin\alpha)}}{\pm\, j\sin\alpha - 4\cos\alpha} \;+\; O\;\left(\frac{1}{L^3}\right) \tag{179}$$

where the $(\pm)$ corresponds to $\binom{1}{2}$. Similarly,

$$< H_n^{(1)}(2k_1\,\rho_m)\, H_n^{(2)}\,(2k_1\,\rho_m) >_{\rho_m} \;\sim\; \frac{2\pi}{L\,\sin\alpha} \;+\; O\;\left(\frac{1}{L^3}\right) \tag{180}$$

Hence, from eq. (172)

$$< J_n^2\,(2k_1\rho_m) >_{\rho_m} \;\sim\; \frac{\pi}{L}\; \left[ \frac{1}{\sin\,\alpha} \;+\; \frac{1}{[\,\sin^2\alpha + 16\cos^2\alpha\,]^{1/2}} \right.$$

$$\left. e^{-4L\cos\alpha}\,\cos\,(2L\,\sin\alpha - n\pi + \beta) \right] , \;\; \beta = \tan^{-1}\left[\,\frac{1}{4}\,\tan\alpha\,\right] \tag{181}$$

A substantial simplification occurs if

$$4L\cos\alpha \,\equiv\, 8k_1^2\;\sigma_\rho^2 \;>>\; 1 \tag{182}$$

The last term may simply be omitted owing to the exponential decay resulting in

$$< J_n^2 (2k_1 \rho_m) >_{\rho_m} \sim \frac{\pi}{2k_1 \bar{\rho}_m} \tag{183}$$

which is independent of n. Hence, in the limit $k_1 \sigma_\rho >> 1$ the normalized spectrum (167) now reduces to

$$I_E(\omega) = \frac{\pi^2}{k_1 \bar{\rho}_m} \left\{ \delta(\omega) + \sum_{n=1}^{\infty} \frac{1}{n} \left[ P\left(\frac{\omega}{n}\right) + P\left(-\frac{\omega}{n}\right) \right] \right\} \tag{184}$$

The asymptotic expansions (179) (180) presumed not only the largeness of L with respect to unity but also with respect to n. In the case where the series (167) does not converge at a sufficiently rapid rate the results (179) (180) must be reconsidered. The asymptotic analysis must allow for large values of n. The saddle-point condition and the corresponding contributions are modified as indicated next. Let,

$$\hat{Q} \equiv jn(\varphi_1 + \varphi_2) - L[j \sin \alpha (\sin \varphi_1 + \sin \varphi_2) + \cos \alpha (\sin \varphi_1 + \sin \varphi_2)^2] \tag{185}$$

hence,

$$\frac{\partial \hat{Q}}{\partial \varphi_1} = jn - L[j \sin \alpha \cos \varphi_1 + 2 \cos \alpha (\sin \varphi_1 + \sin \varphi_2) \cos \varphi_1] \tag{186}$$

and

$$\frac{\partial^2 \hat{Q}}{\partial \varphi_1^2} = -L[-j \sin \alpha \sin \varphi_1 + 2 \cos \alpha (\cos^2 \varphi_1 - \sin^2 \varphi_1 - \sin \varphi_2 \sin \varphi_1)] \tag{187}$$

The saddle-point conditions are defined by

$$\frac{\partial \hat{Q}}{\partial \varphi_1} \bigg|_{\varphi_{1s}, \varphi_{2s}} = \frac{\partial \hat{Q}}{\partial \varphi_2} \bigg|_{\varphi_{1s}, \varphi_{2s}} = 0 \tag{188}$$

63

We specifically look for solutions of eqs. (188) subject to the constraint

$$\varphi_{1s} = -\varphi_{2s} \tag{189}$$

which selects the unique combination of $\varphi_{1s}$ and $\varphi_{2s}$ giving rise to contributions which are not exponentially small. Such a solution indeed exists and is given (via eq. (186)) by

$$jn - jL \sin \alpha \, \cos \frac{\varphi_{1s}}{2} = 0 \tag{190}$$

or

$$\cos \frac{\varphi_{1s}}{2} = \frac{n}{L \sin \alpha} \;, \quad \sin \frac{\varphi_{1s}}{2} = \pm \sqrt{1 - \left(\frac{n}{L \sin \alpha}\right)^2} \tag{191}$$

The substitution of eq. (191) into (187) results in,

$$\left. \frac{\partial^2 Q}{\partial \varphi_1^2} \right|_{\varphi_{1s} = -\varphi_{2s}} = -L \left[ \mp j \sin \alpha \sqrt{1 - \frac{n^2}{L^2 \sin^2 \alpha}} + 2 \cos \alpha \, \frac{n^2}{L^2 \sin^2 \alpha} \right] \tag{192}$$

and

$$\left. \frac{\partial^2 Q}{\partial \varphi_1^2} \; \frac{\partial^2 Q}{\partial \varphi_2^2} \right|_{\varphi_{1s} = -\varphi_{2s}} = L^2 \left[ \sin^2 \alpha \left( 1 - \frac{n^2}{L^2 \sin^2 \alpha} \right) + 4 \cos^2 \alpha \, \frac{n^4}{L^4 \sin^4 \alpha} \right] =$$

$$4 k_1^2 \, \bar{\rho}_m^2 \, - n^2 + n^4 \left( \frac{\sigma_\rho}{\bar{\rho}_m} \right)^4 \tag{193}$$

Therefore,

$$\langle J_n^2 \, (2 k_1 \, \rho_m) \rangle_{\rho_m} \sim \frac{\pi}{\sqrt{4 k_1^2 \, \bar{\rho}_m^2 \, - n^2 + n^4 \left( \frac{\sigma_\rho}{\bar{\rho}_m} \right)^4}} \tag{194}$$

and substitution into eq. (167) results in

$$I_E(\omega) \sim \frac{\pi^2}{k_1 \bar{\rho}_m} \delta(\omega) + 2\pi^2 \sum_{n=1}^{\infty} \frac{P\left(\frac{\omega}{n}\right) + P\left(-\frac{\omega}{n}\right)}{n \sqrt{4k_1^2 \bar{\rho}_m^2 - n^2 + n^4 \left(\frac{\sigma_\rho}{\bar{\rho}_m}\right)^4}} \quad (195)$$

An exact evaluation of $<J_n^2(2k_1 \rho_m)>_{\rho_m}$ is possible for a presumed Rayleigh distributed variable $\rho_m$. One has

$$<J_n^2(2k_1 \rho_m)>_{\rho_m} = \int_{-\infty}^{\infty} d\rho_m \; P(\rho_m) \; J_n^2(2k_1 \rho_m)$$

$$\frac{1}{\hat{\rho}_m^2} \int_0^{\infty} d\rho_m \; \rho_m \; J_n^2(2k_1 \rho_m) \; e^{-\frac{\rho_m^2}{2\hat{\rho}_m^2}} = I_n(4k_1^2 \hat{\rho}_m^2) \; e^{-4k_1^2 \hat{\rho}_m^2} \quad (196)$$

where $\hat{\rho}_m$ denotes the value of $\rho_m$ at the peak of $P(\rho_m)$.

Hence, via eq. (167)

$$I_E(\omega) = 2\pi \; I_o(4k_1^2 \hat{\rho}_m^2 \; e^{-4k_1^2 \hat{\rho}_m^2} \; \delta(\omega) + 2\pi \sum_{n=1}^{\infty} \frac{1}{n} I_n(4k_1^2 \hat{\rho}_m^2) \; e^{-4k_1^2 \hat{\rho}_m^2}[P(\frac{\omega}{n}) + P(-\frac{\omega}{n})]$$

$$(197)$$

which reduces to the results given in eqs. (170) and (184) in the respective asymptotic limits.

The clutter spectrum given by eq. (197) again indicates a DC component at $\omega = o$ plus continuous AC spectrum with the appropriate interchange between these components to conserve energy as the factor $4k_1^2 \hat{\rho}_m^2$ is varied. $I_E(\omega)$ as given by eq. (197) is normalized for unit total clutter power. Hence,

$$P_T = P_{DC} + P_{AC} = \frac{1}{2\pi} \int_{-\infty}^{+\infty} I_E(\omega) \; d\omega = 1 \quad (198)$$

The DC clutter power is

$$P_{DC} = I_o \, (4k_1^2 \, \hat{\rho}_m^2) \, \epsilon^{-4k_1^2 \, \hat{\rho}_m^2} \qquad (199)$$

Hence, the AC clutter power is given by

$$P_{AC} = P_T - P_{DC} = 1 - I_o \, (4k_1^2 \, \hat{\rho}_m^2) \, \epsilon^{-4k_1^2 \, \hat{\rho}_m^2} \qquad (200)$$

Note that this is true, independent of the specific form of the density function of self-resonant frequencies $P(\Omega)$. Figure 12 is a plot of the ratio of AC clutter power to DC clutter power as a function of the parameter $\hat{\rho}_m / \lambda$. For large displacements, this ratio is proportional to $\hat{\rho}_m / \lambda$.

Figure 13 depicts a measured clutter spectrum at UHF ($\lambda = 0.69$ m) under low wind conditions. All of the measured spectra were characterized by a resonant peak at approximately 0.4 Hz. The linear slope (db vs. log frequency) of the observed low wind spectra above this peak suggests a power law representation for $P(\Omega)$ of the form

$$P(\Omega) = \frac{a \, (\Omega / \Omega_o)^p}{1 + b \, (\Omega/\Omega_o)^q} \qquad (201)$$

(see eq. (171)). A good fit to the tail of the low wind spectrum was obtained with parameters chosen such that $q - p \approx 5.7$. Alternative choices for $P(\Omega)$, such as a Rayleigh distribution or the Maxwell distribution included in Fig. 10, can not accurately produce the observed low wind clutter spectra.

The power law distribution which matched the low wind UHF spectra was then used in eq. (197) to predict clutter spectra at both UHF and L-band carrier frequencies for higher wind conditions. These results are illustrated by Fig. 14. The experimental data at the two frequencies was obtained simultaneously from a common range cell. It is seen that the power law distribution
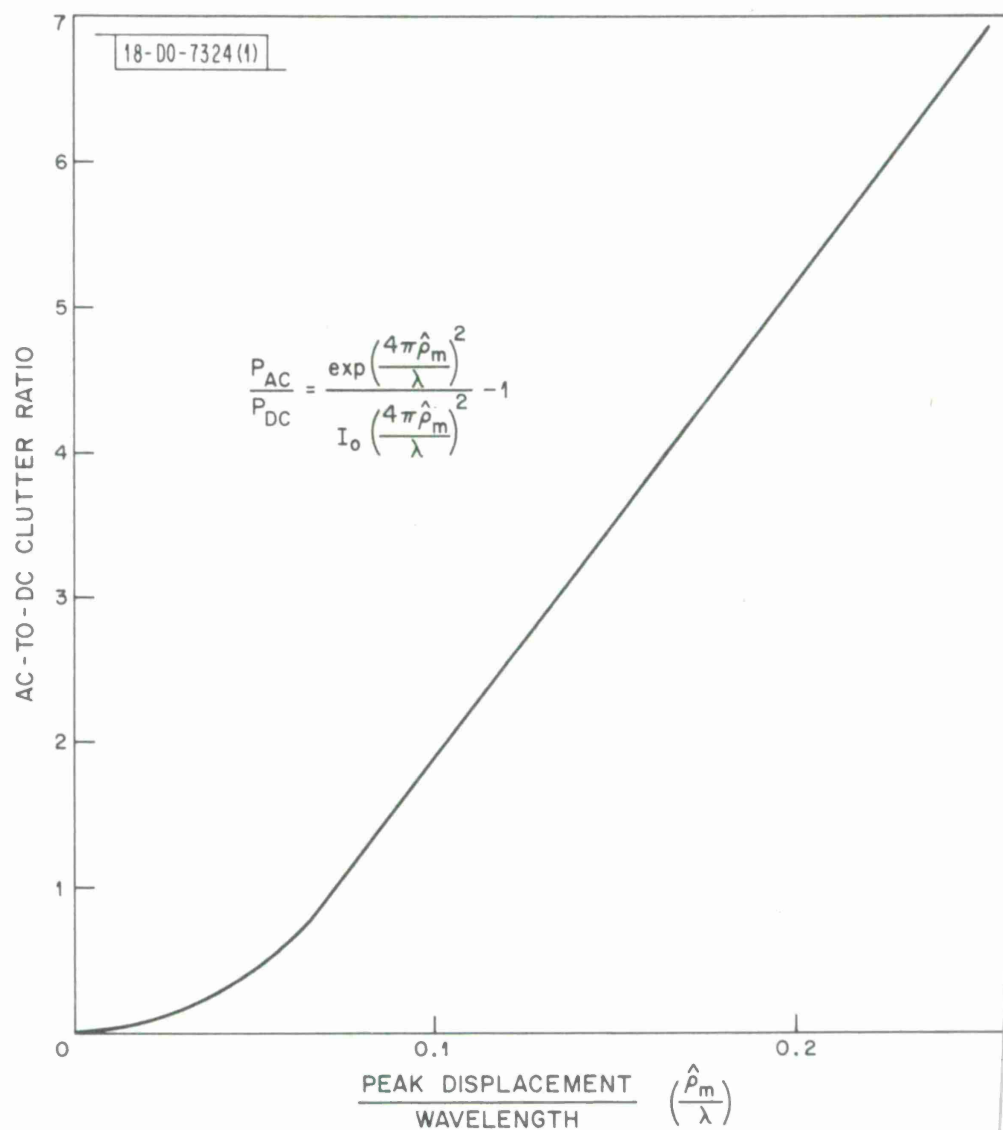
66

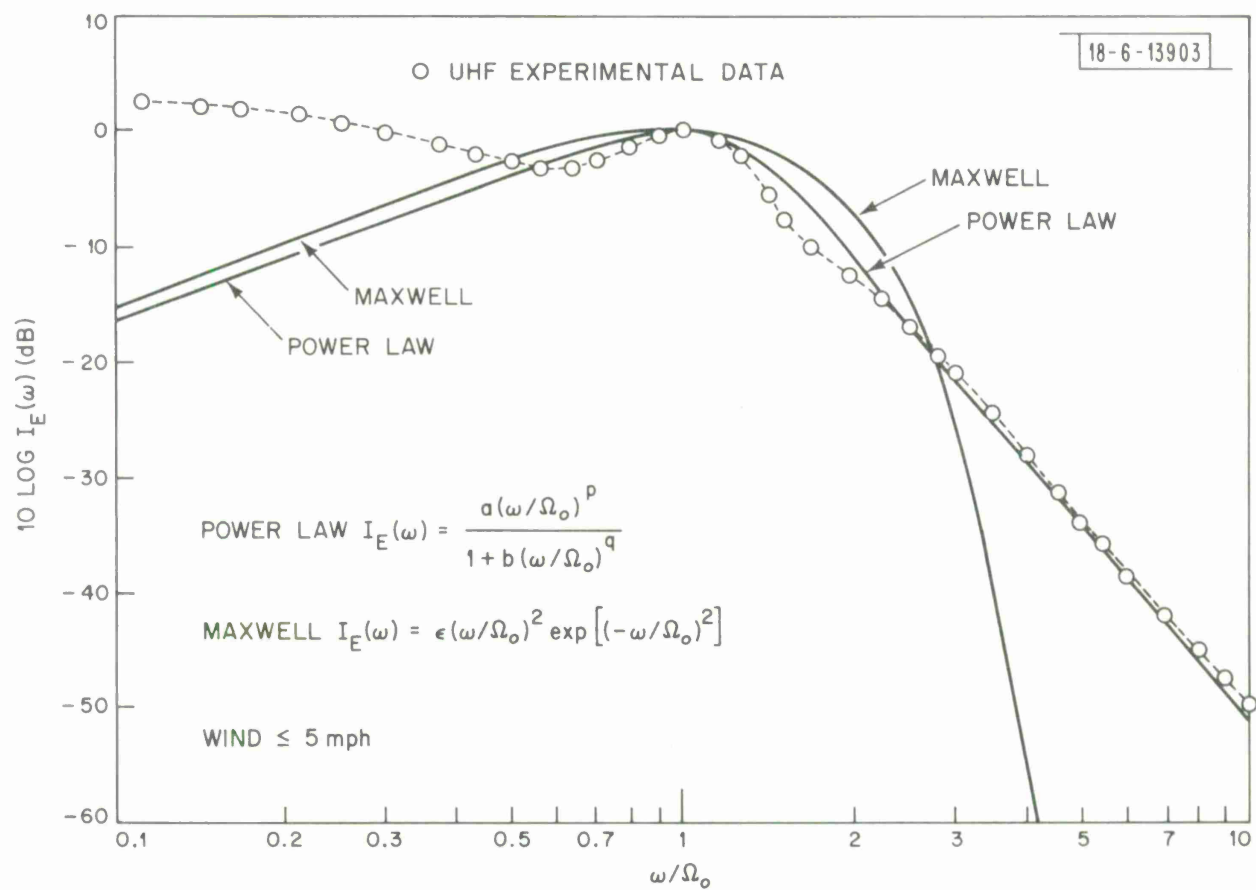Fig. 12.  AC-to-DC clutter ratio for Rayleigh distributed displacements.

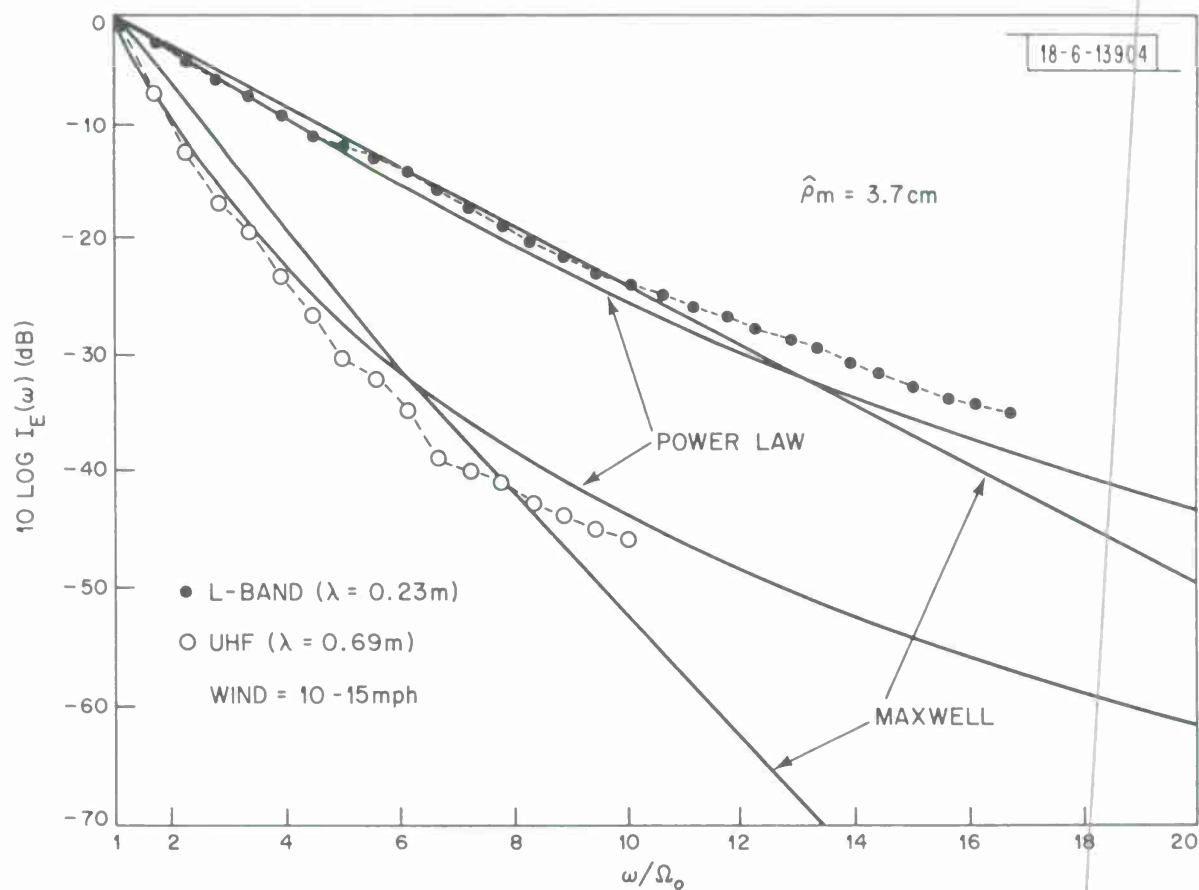Fig. 13.   Low wind clutter spectra.   Deflections Rayleigh distributed.

Fig. 14. Moderate wind clutter spectra. Deflections Rayleigh distributed.

69

with a deflection parameter of $\hat{\rho}_m$ = 3.7 cm which quite accurately matches the observed L-band spectrum also predicts reasonably well the observed UHF spectrum.

The Maxwell distribution of $P(\Omega)$, which was seen to be a poor choice under low wind conditions, yields much more reasonable results with stronger winds. This suggests that the higher wind spectra are less sensitive to the distribution of self-resonant frequencies of the scatterers.

It should be observed that the distribution of $\rho_m$ characterized by the parameter $\hat{\rho}_m$ may depend upon the frequency of the incident radiation. As the frequency increases, smaller-scale scattering centers start to effectively participate in the scattering process. It is anticipated that these smaller constituents will move with larger amplitudes and thus thend to increase $\hat{\rho}_m$. The trend is reversed as the frequency decreases. While the qualitative observation is simple, no satisfactory quantitative procedure has been established.

# APPENDIX

The objective of this Appendix is to prove the validity of the relation:

$$\text{Var } P_r \equiv < [ P_r - <P_r> ]^2 = <P_r>^2 \tag{A1}$$

under the constraints of single-scatter theory and the presumed largeness (compared to the correlation length) of the scattering volume.

Let

$$\underline{E}_1 = \text{Re} [ \Delta \underline{E}_{si} ], \quad \underline{E}_2 = \text{Im} [ \Delta \underline{E}_{si} ] \tag{A2}$$

The largeness of $\Delta V_i$ in eq. (118) assures (via the central limit theorem) the normal character of $\Delta \underline{E}_{si}$ (which is therefore completely defined by its two-point correlations). Upon forming the expression $<\Delta \underline{E}_{si} \cdot \Delta \underline{E}_{si} >$ (via eq. (118)), transforming the resulting double integral (say over $\underline{r}_1$ and $\underline{r}_2$) into the center of mass ($R = \frac{1}{2} (\underline{r}_1 + \underline{r}_2)$) and relative ($\hat{\underline{r}} = \underline{r}_1 - \underline{r}_2$) coordinate systems and further separating the horizontal coordinates from the vertical, one obtains:

$$<\Delta \underline{E}_{si} (\underline{r}, t) \cdot \Delta \underline{E}_{si} (\underline{r}', t+\tau)> = \frac{\omega_o^4 \mu_o^2 z^2 z'^2}{\pi^2 (\eta^2 - 1)^2 \rho_o^8} \; e^{jk_1 \frac{z^2 + z'^2}{2} - j2k_1 (\rho_o + \rho_o') F^2(\varphi_i)}$$

$$\int_{\Delta V_i} d^3 \hat{r} \; C(\hat{\underline{r}}, \tau) \int_{-h}^{o} dZ \; \gamma(z_1) \gamma(z_2) e^{[j2k_1 \sqrt{1-\eta^2} + \frac{2\alpha}{\sqrt{1-\eta^{-2}}}] (z_1 + z_2)}$$

$$\left[ \int_{\Delta S_i} d^2 \bar{\rho} \; e^{j4k_1 \underline{\rho} oi \cdot \bar{\rho}} \right] \tag{A3}$$

It is the bracketed term in eq. (A3) which is of special interest, since

$$\lim_{\Delta S_i \to \infty} \int_{\Delta S_i} d^2 \bar{\rho} \; e^{j4k_1 \underline{\rho} oi \cdot \bar{\rho}} = (2\pi)^2 \delta (4k_1 \underline{\rho}_{oi}) \tag{A4}$$

71

Hence, the largeness of $\Delta S_i$ is measured on the scale of the wavelength of the incident radiation (rather than the correlation distance characterizing $\epsilon(\underline{r}, t)$. It follows that,

$$<\Delta \underline{E}_{si} (\underline{r}, t) \cdot \Delta \underline{E}_{si} (\underline{r}', t+\tau)> = 0 \tag{A5}$$

or

$$<\underline{E}_1 (\underline{r}, t) \cdot \underline{E}_1 (\underline{r}', t+\tau)> = <\underline{E}_2 (\underline{r}, t) \cdot \underline{E}_2 (\underline{r}', t+\tau)> \tag{A6}$$

and

$$<\underline{E}_1 (\underline{r}, t) \cdot \underline{E}_2 (\underline{r}', t+\tau)> = -<\underline{E}_1 (\underline{r}', t+\tau) \cdot \underline{E}_2 (\underline{r}, t)> \tag{A7}$$

Although one can continue with the treatment of the two-point statistics, we restrict ourselves to the discussion of the one point statistics relevant to the proof of eq. (A1). With $\underline{r} = \underline{r}'$ and $\tau = 0$ in eqs. (6, 7) it follows that:

$$<E_1^2> = <E_2^2> = \sigma_E^2, \quad <\underline{E}_1 \cdot \underline{E}_2> = 0 \tag{A8}$$

Hence, the joint distribution is given by

$$P(E_1, E_2) = \frac{1}{2\pi \sigma_E^2} e^{-\frac{E_1^2 + E_2^2}{2\sigma_E^2}} \tag{A9}$$

Or in terms of the amplitude and phase, with

$$A = [E_1^2 + E_2^2]^{1/2}, \quad \varphi = \tan^{-1} \frac{E_2}{E_1} \tag{A10}$$

one obtains

$$P(A, \varphi) = \frac{A}{2\pi \sigma_E^2} e^{-\frac{A^2}{2 \sigma_E^2}} U(A) \tag{A11}$$

For the Rayleigh distribution (A11) it follows:

$$<A^2> = 2 \sigma_E^2, \quad <A^4> = 8 \sigma_E^4 \qquad (A12)$$

Hence (with S denoting the Poynting vector),

$$\text{Var } S = <[S - <S>]^2> = \frac{1}{4} \frac{\epsilon_o}{\mu_o} <[A^2 - <A^2>]^2> =$$

$$\frac{1}{4} \frac{\epsilon_o}{\mu_o} [<A^4> - <A^2>^2] = \frac{\epsilon_o}{\mu_o} \sigma_E^4 = <S>^2 \qquad (A13)$$

where eq. (A12) was utilized. Eq. (A1) results.

# REFERENCES

1    F. C. Karal and J. B Keller, "Elastic, Electromagnetic, and Other Waves in a Random Medium," J. Math. Phys. $\underline{5}$, 537-547, (1964).

2    A. T. Bharucha-Reid (Editor), "Wave Propagation in Random Media," in Probablistic Methods in Applied Mathematics, Vol. I (Academic Press, New York, 1968), pp. 75-198.

3    S. Rosenbaum, "An Effective Medium and Plane Wave Dispersion Relation Relevant to the Mean Wave Propagation in a Forest Environment," ECOM Report (1969).

4    T. Tamir, "On Radio-Wave Propagation in Forest Environments," IEEE Trans. Antennas Propag. $\underline{AP-15}$, 806-817 (1967).

5    D. L. Sachs, P. J. Wyatt, "A Conducting-Slab Model for Electromagnetic Propagation Within a Jungle Medium," Radio Sci. $\underline{3}$, 125-134 (1968).

6    R. S. Ruffine and D. A. deWolf, "Cross-Polarized Electromagnetic Backscatter from a Turbulent Plasma," J. Geophys. Res. $\underline{70}$, 4313-4321 (1965).

## DOCUMENT CONTROL DATA - R&D

*(Security classification of title, body of abstract and indexing annotation must be entered when the overall report is classified)*

| 1. ORIGINATING ACTIVITY (Corporate author) | 2a. REPORT SECURITY CLASSIFICATION |
|---|---|
| Lincoln Laboratory, M.I.T. | Unclassified |
| | 2b. GROUP |
| | None |

3. REPORT TITLE

Clutter Return from Vegetated Areas

4. DESCRIPTIVE NOTES *(Type of report and inclusive dates)*

Technical Note

5. AUTHOR(S) *(Last name, first name, initial)*

Rosenbaum, Shalom and Bowles, Leonard W.

| 6. REPORT DATE | 7a. TOTAL NO. OF PAGES | 7b. NO. OF REFS |
|---|---|---|
| 10 September 1971 | 82 | 6 |

| 8a. CONTRACT OR GRANT NO.   F19628-70-C-0230 | 9a. ORIGINATOR'S REPORT NUMBER(S) |
|---|---|
| b. PROJECT NO.   ARPA Order 1559 | Technical Note 1971-34 |
| | 9b. OTHER REPORT NO(S) *(Any other numbers that may be assigned this report)* |
| c.   649L | ESD-TR-71-138 |
| d. | |

10. AVAILABILITY/LIMITATION NOTICES

Approved for public release; distribution unlimited.

| 11. SUPPLEMENTARY NOTES | 12. SPONSORING MILITARY ACTIVITY |
|---|---|
| None | Air Force Systems Command, USAF Advanced Research Projects Agency, Department of Defense |

13. ABSTRACT

The objective of this report is the presentation of an analytical-stochastic model capable of predicting relevant statistical scattering features of electromagnetic waves propagating within vegetated environments. The propagation phenomena are described by formulating the scattering associated with random permittivity fluctuations superimposed on a lossy deterministic background slab. The mean backscattered power, its variance and one-point distribution are calculated. The spectral characteristics of clutter from windblown foliage are investigated using two models; one presuming the velocity field to constitute a multivariate normal process and another presuming the scatterer's motion to be quasi-harmonic over limited time segments.

14. KEY WORDS

electromagnetic waves
clutter
propagation phenomena

scattering
spectral characteristics